

Review

Organic Light-Emitting Diodes with Ultrathin Emitting Nanolayers

Yubu Zhou ¹, Huayu Gao ¹, Jing Wang ², Fion Sze Yan Yeung ², Shenghuang Lin ³ , Xianbo Li ¹, Shaolin Liao ^{1,4} , Dongxiang Luo ^{5,*}, Hoi Sing Kwok ² and Baiquan Liu ^{1,*} ¹ School of Electronics and Information Technology, Sun Yat-sen University, Guangzhou 510275, China² State Key Laboratory on Advanced Displays and Optoelectronics Technologies, Department of Electronic and Computer Engineering, The Hong Kong University of Science and Technology, Hong Kong 999077, China; eefion@ust.hk (F.S.Y.Y.)³ Songshan Lake Materials Laboratory, Dongguan 523808, China⁴ Department of Electrical and Computer Engineering, Illinois Institute of Technology, Chicago, IL 60616, USA⁵ Huangpu Hydrogen Innovation Center/Guangzhou Key Laboratory for Clean Energy and Materials, School of Chemistry and Chemical Engineering, Guangzhou University, Guangzhou 510006, China

* Correspondence: luodx@gzhu.edu.cn (D.L.); liubq33@mail.sysu.edu.cn (B.L.)

Abstract: Organic light-emitting diodes (OLEDs) are promising for displays and lighting technologies because of their excellent advantages, such as high efficiency, high luminance, low power consumption, light weight, and flexibility. In recent years, ultrathin emitting nanolayers (UENs) have been used to develop OLEDs without the doping technique, which can simplify device structure, reduce material loss, achieve good exciton utilization, and realize comparable performance to doped devices such as the external quantum efficiency of 28.16%, current efficiency of 63.84 cd/A, and power efficiency of 76.70 Lm/W for white OLEDs. In this review, we comprehensively summarize the recent progress in the field of UEN-based OLEDs. Firstly, the host–guest-doped OLEDs and doping-free UEN-based OLEDs are compared. Then, various effective approaches for designing UEN-based OLEDs are presented, including both monochromatic and white devices. In particular, the properties of materials, the design of device structures, and the main working mechanisms of UEN-based OLEDs are highlighted. Finally, an outlook on the future development of UEN-based OLEDs is provided.

Keywords: organic light-emitting diode; ultrathin emitting nanolayer; efficiency; doping-free; simplicity



Citation: Zhou, Y.; Gao, H.; Wang, J.; Yeung, F.S.Y.; Lin, S.; Li, X.; Liao, S.; Luo, D.; Kwok, H.S.; Liu, B. Organic Light-Emitting Diodes with Ultrathin Emitting Nanolayers. *Electronics* **2023**, *12*, 3164. <https://doi.org/10.3390/electronics12143164>

Academic Editors: Aobo Ren, Kai Shen and Keren Li

Received: 15 June 2023

Revised: 11 July 2023

Accepted: 14 July 2023

Published: 21 July 2023



Copyright: © 2023 by the authors. Licensee MDPI, Basel, Switzerland. This article is an open access article distributed under the terms and conditions of the Creative Commons Attribution (CC BY) license (<https://creativecommons.org/licenses/by/4.0/>).

1. Introduction

In 1987, Tang et al. reported the first organic light-emitting diodes (OLEDs) with an external quantum efficiency (EQE) of 1%, setting off an OLED research boom [1]. OLEDs have become one of the most promising display technologies due to their advantages of self-emissivity, high efficiency, high luminance, high contrast ratio, and flexibility [2–7]. A reasonable emitting layer has been well demonstrated to be the key to achieving high device performance [8–16]. However, host–guest doping techniques are commonly used to produce emitting layers in OLEDs in order to solve the problems of molecular aggregation and exciton quenching. As a result, doping techniques can improve the luminescence efficiency, broaden the design flexibility of devices, and inhibit device aging [17,18]. Nevertheless, there are still many limitations for doping techniques such as high-precision doping, high requirements for the host material, and high manufacturing costs, especially for the complex device structure of white OLEDs (WOLEDs) requiring the incorporation of two or more emitting layers [19–24]. Due to the limitations of traditional doping technology, doping-free organic light-emitting diodes (DF-OLEDs) have gradually attracted the attention of researchers, and OLEDs comprising ultrathin emitting nanolayers (UENs) have been extensively studied over the past few years.

In UEN-based OLEDs, as the name implies, the emitting layer is usually very thin (e.g., <1 nm) compared to the doped OLEDs. The exploitation of UENs does not have to use doping technology since it can form a similar co-doping effect with adjacent layers, which makes the device structure and fabrication process more simplified [25–27]. In addition, the device design becomes more flexible, and the material consumption and manufacturing costs are lowered [28,29]. Nowadays, UENs can achieve high electroluminescence (EL) performance. For example, the EQE of UEN-based OLEDs can exceed 20%, and the color rendering index (CRI) can exceed 90 [30,31].

In this review, we first compare traditional host–guest doping structures with the UEN-based technique to clarify the characteristics of UEN-based OLEDs. Then, the latest progress in research on OLEDs with UENs is reviewed in detail, including both monochromatic and white devices. Finally, we present our views on the future development of OLEDs with UENs.

2. Comparison of Host–Guest Doping Structures and Doping-Free UEN-Based OLEDs

2.1. Host–Guest Doping Structures

The conventional host–guest doping system combines the host material with various high-efficiency guest emitters, obtaining high efficiency and different light colors [32–35]. However, on one hand, if the doping concentration is too low, the distance between the host and guest molecules would be larger than the energy transfer radius, and the exciton on the host molecule will first spread to another host molecule instead of the doped guest molecule, which will lead to energy loss [36–38]. On the other hand, if the doping concentration is too high, the π - π stacking interaction of the doped guest molecule will be enhanced, leading to concentration quenching [39,40]. Because of the demand for energy transfer, the host material is required to have a high triplet (T1) energy level, suitable lowest unoccupied molecule orbital (LUMO) and highest occupied molecule orbital (HOMO) energy levels matching the carrier transport layer, and good carrier transport capability [41–43]. In particular, the triplet energy of host materials is required to be higher than that of guests in both phosphorescence and thermally activated delayed fluorescence (TADF) OLEDs because TADF materials are capable of harvesting triplet excitons by utilizing the reverse intersystem crossing (RISC) mechanism. In addition, the co-evaporation technology, which is used to construct a host–guest doping structure, has some shortcomings such as low material utilization, unsatisfactory reproducibility for mass production, high demand for customization of equipment, and high manufacturing cost of devices. Hence, the commercial development of doped OLEDs is still challenging [44–47]. In view of the above limitations, the development of more economical and environmentally friendly DF-OLEDs is helpful.

2.2. UEN-Based OLEDs

UEN-based OLEDs originated from the study of sub-monolayer materials inserted into OLEDs. Initially, researchers inserted light-emitting or electrode materials such as 5,6,11,12-tetraphenylanthracene (Rubrene), [2-methyl-6-[2-(2,3,6,7-tetrahydro-1H, red fluorescent dye 5H-benzo[*ij*]quinolizin-9-yl)ethenyl]-4H-pyran-4-ylidene]propane-dinitrile, quinacridone, Cs, and LiF into OLEDs in the form of sub-monolayers to obtain the EL spectra and improve the device performance [48–54]. It was found that the introduction of a sub-monolayer does not cause significant changes in carrier behaviors. In addition, the inserted ultrathin luminescent material film is not continuous; its molecules are scattered in islands on the rough adjacent layers (Figure 1), leading to molecular aggregation decreasing and concentration quenching. It presents a special doping effect (two-dimensional), which is similar to the conventional host–guest system (three-dimensional). The materials on both sides of the introduced ultrathin layers can be considered as the host, while the inserted ultrathin layers can be regarded as the guest. Compared with the complex doped OLEDs, UEN-based OLEDs have many advantages such as simple structure, avoiding the complicated and expensive co-evaporation technology, and the ability to precisely control

the thickness of UENs by sensor detection. Based on the above advantages, UEN-based OLEDs are a promising direction for the development of DF-OLEDs. Hence, researchers use more and more emitting materials as UENs, and the study of UEN-based OLEDs has emerged. So far, it is feasible to achieve high EL performance for UEN-based OLEDs, which can be comparable to conventional doped OLEDs. Additionally, it should be pointed out that phosphorescence emitters are generally adopted to boost the efficiency of UEN-based OLEDs since both singlet and triplet excitons can be harvested. Thus, among the reported representative UEN-based OLEDs, phosphorescence OLED devices are mostly focused on to date.

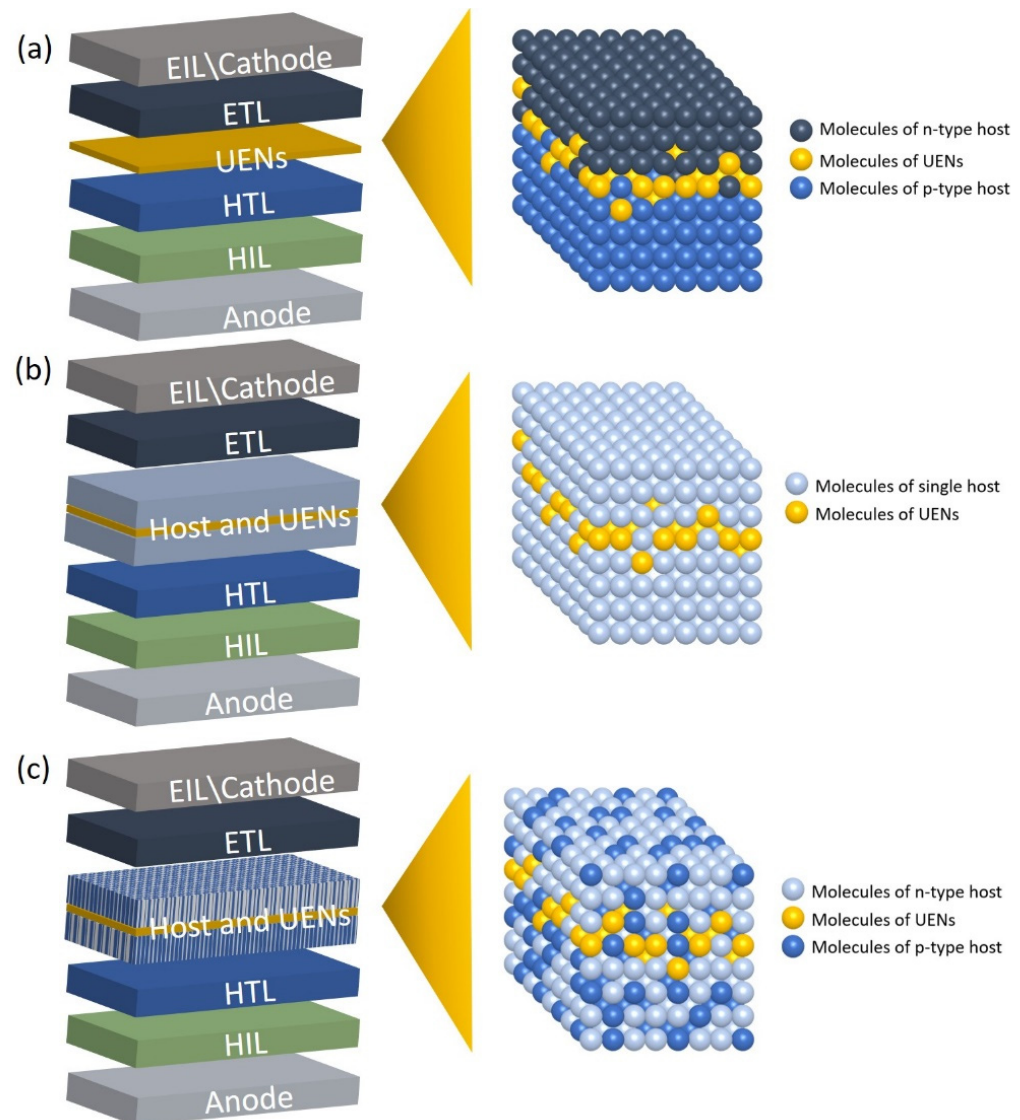


Figure 1. Schematic device structure and emitting layer molecule distribution of OLEDs with UENs inserted into (a) heterojunction interfaces, (b) single host materials, and (c) mixed host materials. HIL, HTL, ETL, and EIL are hole injection layer, hole transport layer, electron transport layer, and electron injection layer, respectively.

3. Progress in UEN-Based OLED Research

A main research purpose in the study of UEN-based structures is to develop low-cost and high-performance DF-WOLEDs. Since monochromatic emission is the basis of white colors, the development of high-performance monochromatic OLEDs using UEN structures has also been reported [55–58]. Therefore, in this section, the progress in research on monochromatic OLEDs based on UEN structures is first stated. Then, the progress

in research on WOLEDs based on UEN structures is introduced in detail. The detailed performance of representative UEN-based OLEDs is shown in Table 1.

3.1. UEN-Based Monochromatic OLEDs

3.1.1. UEN-Based Red OLEDs

Currently, it is relatively easy to achieve high efficiency for red OLEDs. Therefore, the utilization of UEN structures is a feasible way to develop high-performance red OLEDs. Additionally, red UENs can be used as a basis to develop WOLEDs or to verify the electroluminescent properties of red-emitting materials due to the low cost.

To solve the problem of color purity deterioration and concentration quenching in a conventional doping system, Xu et al. used UENs of 4-(dicyanomethylene)-2-t-butyl-6-(1,1,7,7-tetramethyljulolidyl-9-enyl)-4H-pyran (DCJTb) and Rubrene to confine charges and excitons [59]. The device structure was indium tin oxide (ITO)/N,N'-bis-(1-naphthyl)-N,N'-diphenyl-1,10-biph-enyl-4,40-dia-mine (NPB) (48 nm)/Rubrene (0.05 nm)/NPB (1 nm)/DCJTb (0.1 nm)/NPB (1 nm)/Rubrene (0.05 nm)/tri-(8-hydroxyquinoline) aluminum Alq₃ (40 nm)/LiF (0.3 nm)/Al (150 nm). Their best device obtained the maximum current efficiency (CE) of 5.6 cd/A, luminance of 21,525 cd/m², and CIE coordinates of (0.617, 0.379). It was quite a high performance at that time. This representative work took place in the early stages of the study of UEN-based OLEDs. It demonstrated some optimization strategies in conventional devices such as confining charges and excitons and the great potential of high-performance UEN-based OLEDs.

In 2015, Xue et al. manufactured UEN-based red OLEDs for the development of WOLEDs, where the structure was ITO/MoO₃ (2 nm)/1,3-bis(carbazol-9-yl)benzene (MCP) (60 nm)/bis(2-methyldibenzo[f,h] quinoxaline)-(acetylacetonate)-iridium(III) [Ir(MDQ)₂(acac)] (X nm)/1,3-bis[3,5-di(pyridin-3-yl)phenyl]benzene (BmPyPhB) (30 nm)/8-hydroxyquinolino lithium (Liq) (1 nm)/Al (100 nm) [60]. The best device obtained high performance with a CE of 19.3 cd/A and power efficiency (PE) of 17.3 Lm/W at 0.1 nm thickness. In 2017, Liu et al. fabricated UEN-based OLEDs with the structure of ITO/MoO₃/1,1-bis[(di-4-tolylamino)phenyl]-cyclohexane (TAPC, 60 nm)/4,4',4''-tri(N-carbazolyl)triphenylamine (TCTA, 5 nm)/4,4'-(naphtho [2,3-c][1,2,5]thiadiazole-4,9-diyl)bis(N,N-diphenylaniline) (NZ2TPA, 0.1 nm)/bis(10-hydroxybenzo[h]quinolino)beryllium (Bebq₂, 50 nm)/LiF (1 nm)/Al. This device structure was used to verify the EL property of the near-infrared emitter NZ2TPA [61]. The results were encouraging, with the maximum EQE of 3.9% at 696 nm and the highest luminance of 6330 cd/m². In 2023, Miao et al. fabricated a high-performance UEN-based red OLED, achieving the peak EQE, CE, and PE of 20.90%, 38.48 cd/A, and 44.78 Lm/W, respectively [36]. The device structure was ITO (180 nm)/MoO₃ (3 nm)/TAPC (x nm)/m-bis(N-carbazolyl)-benzene (MCP) (10 nm)/bis[2-(4,6-difluoro-phenyl)pyridinato-C₂,N](picolino)iridium(III) (Flrpic) (0.40 nm)/2,4,6-tris[3-(diphenylphosphinyl)phenyl]-1,3,5-triazine (PO-T2T) (50 nm)/LiF (1 nm)/Al (100 nm). Although there was no detailed explanation for the high performance, it could be speculated that the reasons were the good confinement of excitons by hole-transporting MCP and electron-transporting PO-T2T and an ideal charge balance at the MCP/PO-T2T interface.

3.1.2. UEN-Based Yellow/Orange OLEDs

In addition to achieving high efficiency, researchers have broadly explored the emission mechanism of devices by fabricating yellow and orange OLEDs based on UEN structures. With such efforts, more insightful mechanisms have been unlocked in recent years.

To discover more emission mechanisms related to UEN-based OLEDs, in 2019, Zhao et al. developed high-performance orange OLEDs with UEN structures [62]. The characteristics and structure of the device with doping-free UENs are shown in Figure 2. The maximum CE, PE, EQE, and luminance could reach 52.0 cd/A, 65.3 Lm/W, 22.8%, and 20,800 cd/m², respectively, in device B2. The specific structure of B2 was ITO/NPB:15%MoO_x (40 nm)/NPB (10 nm)/TCTA (10 nm)/bis(2-phenylbenzothiazolato)(acetylacetonate)iridium [bt₂Ir(acac)] (0.2 nm)/TCTA: TPBi (1:1) (5 nm)/bt₂Ir(acac) (0.2 nm)/TCTA: TPBi (1:1) (5 nm)/bt₂Ir(acac)

(0.2 nm)/TPBi (40 nm)/Liq (1 nm)/Al (120 nm). Compared with the single ultrathin luminescent layer in device B1, whose luminescent layer was $\text{bt}_2\text{Ir}(\text{acac})$ (0.2 nm), they found that the CE, PE, and EQE of the device based on dual luminescent layers were about twice as much as those of the device based on a single ultrathin luminescent layer. They speculated that the high exciton concentration at the TCTA/TPBi interface led to exciton annihilation, and the multi-UEN structure with a spacer layer caused the low-concentration exciton accumulation, making the quenching negligible. This representative work shows the importance of interlayers in achieving high-performance UEN-based OLEDs. The importance of interlayers in UEN-based OLEDs will be discussed in more detail later.

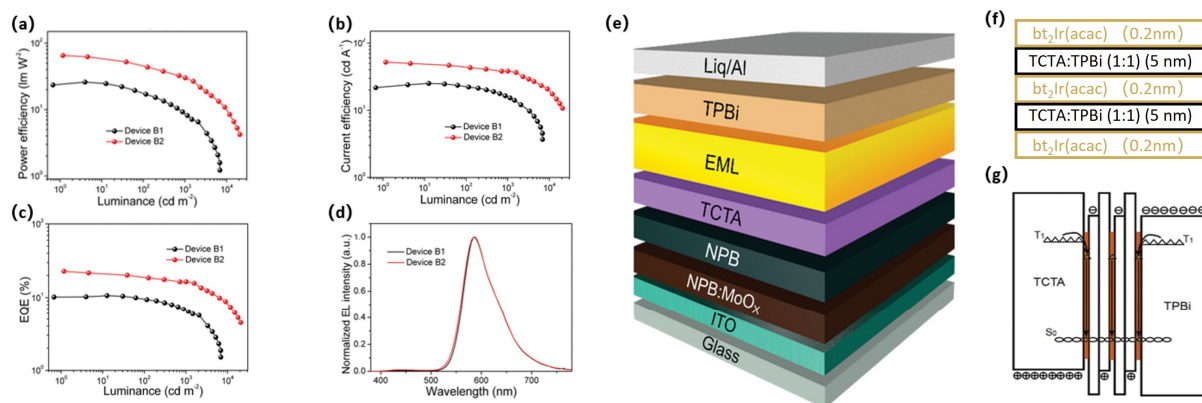


Figure 2. Characteristics of UEN-based OLEDs. (a) Power efficiency (PE), (b) current efficiency (CE), (c) EQE, and (d) EL spectra of devices B1 and B2. (e) The structure of devices. (f) The detailed EML of device B2. (g) Schematic diagram of the emission mechanism of device B2. Reproduced from reference [62], Wiley–Blackwell, 2019 [62].

Xue et al. developed UEN-based orange OLEDs with optimized structures of ITO/MoO₃ (2 nm)/4,4'-N,N'-dicarbazole-biphenyl (CBP) (70 nm)/bis(4-phenylthieno [3,2-c]pyridinato-N,C20) acetylacetonate iridium(III) (PO-01) (X nm)/2,2',2''-(1,3,5-benzinetriyl)-tris(1-phenyl-1-H-benzimidazole) (TPBi) (30 nm)/LiF (0.8 nm)/Al (100 nm), obtaining the CE of 51.2 cd/A at 0.15 nm thickness [60,63]. By changing the position of PO-01 inserted in CBP, they pointed out that the energy was transferred from CBP and TPBi to PO-01, rather than PO-01 capturing the charge exciton formation directly. Wang et al. explored the emission mechanism of exciplex generation by using ultrathin Rubrene emitting layer-based orange OLEDs [64]. The structures were ITO/NPB (30 nm)/TCTA or CBP (10 nm)/Rubrene (0.1, 0.2, 0.4, 0.6 and 0.8 nm)/TPBi (10 nm)/4,7-diphenyl-1,10-phe-nanthroline (Bphen) (40 nm)/Mg: Ag (100 nm). The EL characteristics of TCTA devices with exciplex formation were found to have little effect on the current density by changing the Rubrene thickness, indicating that energy transfer was the main emission mechanism. The authors pointed out that the exciplex could be used to achieve the TADF process, and the EQE of the TCTA devices was 5.3%, which proved the existence of RISC. The current density of CBP devices without exciplex formation decreased significantly with increasing Rubrene thickness, suggesting that the main emission mechanism of the devices was charge trapping.

UEN-based yellow and orange OLEDs also were used to examine the EL performance of newly developed emitting materials. For example, in 2021, Kidanu et al. used a newly proposed platinum complex, called FBNNND, to develop high-performance orange OLEDs and achieved pure yellow emission at the FBNNND thickness of 0.6 nm with a maximum EQE of 20.2% [65].

3.1.3. UEN-Based Green OLEDs

Apart from high-efficiency red OLEDs, researchers' pursuit of high efficiency with UENs lies more in green ones, and some intensive studies about UEN-based green OLEDs have been conducted.

In 2018, Zhang et al. simply positioned the UENs away from the high-concentration exciton formation region to effectively avoid the exciton annihilation due to exciton diffusion region expansion, significantly improving the efficiency decay at high luminance [66]. The characteristics of their devices are shown in Figure 3. The different positions of exciton emission and exciton recombination were the reason for the devices' performance differences. In device D3, they were completely separated, while they were overlapped in devices D1 and D2. The structure of the best-performing device D3 was ITO (180 nm)/MoO₃ (10 nm)/MoO₃: NPB (25%, 35 nm)/NPB (10 nm)/TAPC (5 nm)/TCTA (5 nm)/Bepp₂ (4 nm)/Ir(ppy)₂(acac) (0.2 nm)/Bepp₂ (16 nm)/Bepp₂: Liq (3%, 25 nm)/Liq (1 nm)/Al (150 nm). Its EQE, CE, and PE reached 25.5%, 98.0 cd/A, and 85.4 lm/W at the peak and remained at 24.3%, 92.7 cd/A, 49.3 lm/W at 10,000 cd/m² luminance, respectively. The representative work shows another crucial factor regarding UEN-based OLEDs, namely that the position of UENs should be carefully adjusted for high performance.

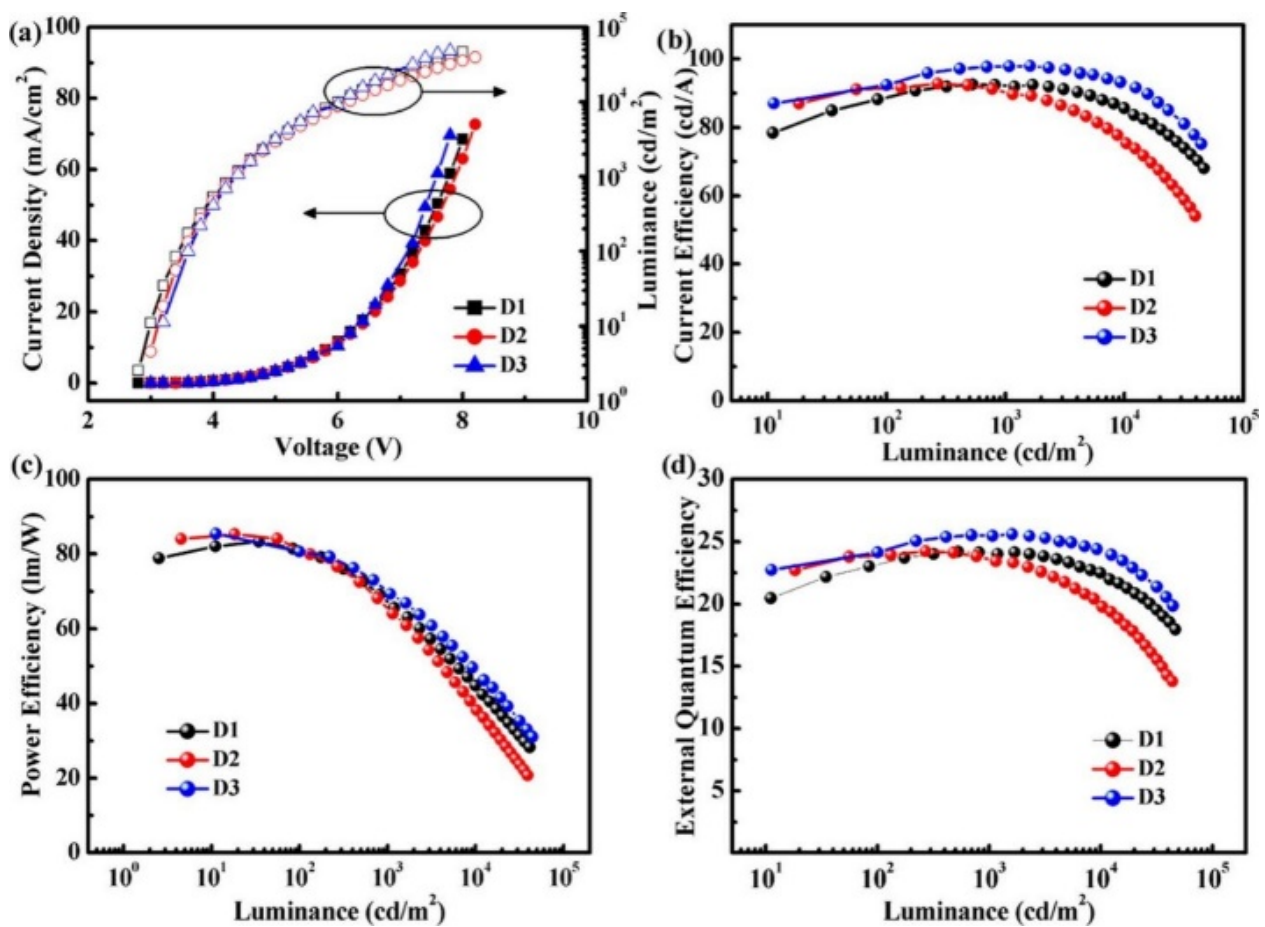


Figure 3. Characteristics of devices D1–D3: (a) current–voltage–luminance, (b) CE–luminance, (c) PE–luminance, and (d) EQE–luminance. Reproduced from reference [65], American Chemical Society, 2018 [66].

Liu et al. used UENs to broaden the exciton complex region, resulting in more efficient energy transfer to the emitter [67]. The specific device structure was ITO/Cs₂CO₃ (1 nm)/BPhen (35 nm)/TPBI (12.5 nm)/emitter (0.5 nm)/MCP (49 nm)/MoO₃ (6 nm)/Al (100 nm), which yielded an EQE of 24.7%. In the same year, Shi et al. realized a high-efficiency green phosphorescent top-emitting OLED with UENs, which had a greater improvement in CE compared with the bottom-emitting device (2.7 times) [68]. It was pointed out that by limiting the emission area at the wave web of the top-emitting OLEDs based on UENs, the micro-cavity effect in the top-emitting device could be better utilized to achieve efficiency improvement. The study also compared single and dual ultrathin layers,

and the dual-ultrathin-layer device could better balance the charge to further improve the efficiency. After optimization, the maximum CE reached 126.3 cd/A for the device structure of Al/MoO₃ (3 nm)/MCP (50 nm)/iridium(III)bis(2-(4-trifluoromethylphenyl)pyridine)tetraphenylimidodi-phosphinate [Ir(tfmppy)₂(tpip)] (0.5 nm)/separate layer/Ir(tfmppy)₂(tpip) (0.5 nm)/TPBi (10 nm)/Bphen (45 nm)/Liq (1 nm)/Al (1 nm)/Ag (22 nm)/MCP (80 nm). In 2017, Xu et al. well integrated the exciplex, tandem, and UEN design concepts [69]. As an excellent result, they achieved high performance with a maximum CE of 135.74 cd/A and EQE of 36.85%. The detailed structure was ITO/1,4,5,8,9,11-hexaazatriphenylene-hexacarbonitrile (HAT-CN) (10 nm)/TAPC (55 nm)/bis[2-(2-pyridinyl-N)phenyl-C](acetylacetonato)-iridium(III) [Ir(ppy)₂(acac)] (0.8 nm)/1,3,5-tris[(3-pyridyl)phen-3-yl]benzene (TmPyPB) (40 nm)/BPhen: LiNH₂ (10 nm, 50% by mole)/HAT-CN (10 nm)/TAPC (55 nm)/Ir(ppy)₂(acac) (0.8 nm)/TmPyPB (40 nm)/Liq (2 nm)/Al (120 nm). The reason for high performance was that the rational device structure allowed the inherent properties of the material to be well utilized, which enabled the effective generation of exciplex, a good charge balance, and the excellent confinement of the exciton complex region.

In 2021, Nanda et al. applied the TADF material DTCBPy to develop high-efficiency UEN-based green OLEDs. The structure of the best-performance device was ITO/HAT-CN (10 nm)/NPB (30 nm)/MCP (20 nm)/DTCBPy (1 nm)/dibenzo[b,d]-thiophene-2,8-diylbis(diphenyl-phosphine oxide) (PPT) (10 nm)/TPBi (50 nm)/LiF (1 nm)/Al (100 nm), and it achieved an approximately 2.7 times higher EQE of 13.5% compared to conventional devices with a 30 nm light-emitting layer, which demonstrated the great potential of TADF for UEN-based OLED development [70]. Also, Kang et al. conducted multiple comparative experiments on HAT-CN/TAPC/TCTA/tris[2-phenylpyridinato-C_{2,N}]iridium(III) [Ir(ppy)₃]/TmPyPB/LiF/Al structures with different thicknesses of the UENs, charge transport layer, and charge injection layer to determine the optimal light-emitting layer thickness of 0.075 nm, ETL thickness of 54 nm, HTL thickness of 80 nm, HIL thickness of 0.25 nm, and EIL thickness of 1 nm [71], which also controlled the optical path length and charge balance. Finally, the highest EQE of 23.8% was achieved by sacrificing the need for optical path length but satisfying the dominant charge balance without the use of tandem structure, new host and transport layer. Recently, Wu et al. also fabricated TADF OLEDs based on UENs with the structure of ITO/TAPC (50 nm)/TCTA (10 nm)/TADF material (tBuCzDBA) (1 nm)/4,6-bis(3,5-di(pyridin-4-yl)phenyl)-2-methylpyrimidine (B4PYMPM) (65 nm)/LiF (1 nm)/Al (100 nm), and the maximum CE, PE, and EQE of the device were 70.2 cd/A, 88.2 Lm/W, and 22.0%, respectively [72]. In addition, 1 nm and 10 nm pure hole and pure electron devices were made for comparison, and it was found that there the 1 nm based device had more balanced charge injection and closer charge mobility, revealing the potential of UENs with low power consumption and cost.

3.1.4. UEN-Based Blue OLEDs

Efficient blue emission is key for achieving high-performance white emission, but unfortunately, there are still relatively few blue OLEDs based on UEN structures at present due to the low efficiency and instability restrictions [73–76].

In addition, most UEN-based blue OLEDs are composed of phosphorescent or TADF emitters. On one hand, blue phosphorescent UENs can harvest both triplet and singlet excitons, ensuring high efficiency. For example, the peak CE of 11.9 cd/A and PE of 9.2 Lm/W were achieved at 0.1 nm thickness with the structure of ITO/MoO₃ (2 nm)/MCP (60 nm)/FIRPic (X nm)/BmPyPhB(30 nm)/Liq (1 nm)/Al (100 nm) [60]. Also, Zhang et al. achieved a CE of 25.5 cd/A, PE of 20.0 Lm/W, and EQE of 13.3% using the structure of ITO/[poly(3,4-ethylenedioxy-thiophene): poly(styrenesulfonic acid)] (PEDOT: PSS) (40 nm)/NPB (40 nm)/TCTA (10 nm)/FIRpic (0.25 nm)/TmPyPB(40 nm)/LiF (100 nm) [77]. By further introducing HAT-CN that can form a charge transfer complex with NPB as the charge generation unit of the tandem device, tandem blue OLEDs with a CE of 53.2 cd/A, PE of 23.4 Lm/W and EQE of 27.8% were realized [78]. Mu et al. fabricated

high-performance blue OLEDs by sandwiching an ultrathin Firpic layer between MCP and TmPyPB [79]. The detailed structure was ITO/PEDOT: PSS/TAPC (30 nm)/TCTA (4 nm)/MCP (5 nm)/Firpic (x nm)/TmPyPB (45 nm)/LiF/Al. The optimal PE of 50 Lm/W and EQE close to 18% were demonstrated. The high performance was attributed to the combined benefits of balancing the fluorescence of the exciplex and the phosphorescence of the Firpic decaying, relieving triplet–triplet annihilation (TTA), and suppressing the diffusion of triplets.

On the other hand, blue TADF UMNs are also able to harness 100% exciton utilization efficiency, guaranteeing high device performance. Miao et al. combined the TADF material with a UEN structure by inserting the UENs into the TADF exciplex interface of MCP and PO-T2T [80].

The detailed work is shown in Figure 4. The ultrahigh-performance blue OLEDs showed the CE, PE, EQE, and luminance of 59.34 cd/A, 74.55 Lm/W, 30.21%, and 8578 cd/m², respectively. The specific structure was ITO (180 nm)/MoO₃ (3 nm)/TAPC (45 nm)/MCP (10 nm)/Firpic (0.40 nm)/PO-T2T (50 nm)/LiF (1 nm)/Al (100 nm). The reason for the ultrahigh performance was the good T₁ energy level design and good utilization of material properties. The T₁ values of MCP and PO-T2T are 2.93 eV and 2.99 eV, respectively, higher than the ones in the MCP/PO-T2T exciplex (2.64 eV). Moreover, the T₁ energy levels of the MCP/PO-T2T exciplex are higher than the energy level of Firpic (2.62 eV). This allowed a good transfer of exciton energy from the MCP/PO-T2T exciplex, where excitons were generated, to Firpic. Furthermore, the excellent balance of charge made the exciplex electrically neutral so that it could avoid triplet excitons and polaron quenching. In addition, the exciplex exhibited the characteristics of TADF. The Forster energy transfer from the exciplex to Firpic was enhanced due to the RISC permitting upconversion from triplets to singlets. The non-radiative transition of triplet excitons generated at the exciplex by TTA was effectively suppressed, and a complete exciton utilization was realized. The representative work showed the validity of introducing multi-functional emitting materials to improve performance.

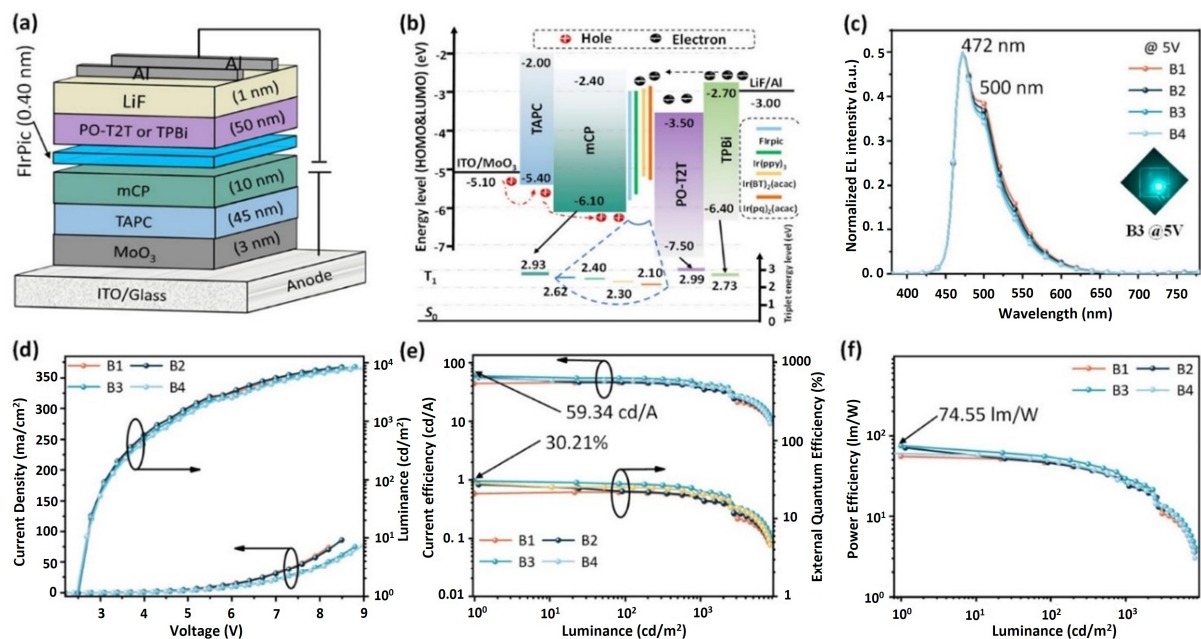


Figure 4. (a) Device structure diagram for all blue devices B1–B4. (b) Schematic energy level diagram for all monochromatic phosphorescent devices in this work. (c) EL spectra for devices B1–B4 at 5 V. (d) CE–voltage–luminance characteristics. (e) CE–luminance–EQE curves. (f) PE–luminance curves for all blue devices B1–B4. Reproduced from reference [80], Elsevier, 2023 [80].

3.2. UEN-Based WOLEDs

The use of UENs to bypass the limitations of doping techniques and develop simple-structure, low-cost, and high-performance WOLEDs is an important goal of researchers. Therefore, there is a wealth of research results in the field of UEN-based WOLEDs. In the early days of research, WOLEDs with UENs were mainly based on traditional orange–blue- or red–blue-emitting materials, called two-color WOLEDs [81–85]. Then, three-color and four-color WOLEDs with more complex device structures were developed in order to simultaneously accomplish high efficiency and high CRI [3,86–88]. In recent years, with the advancement of materials science and understanding of UENs, researchers have been gradually integrating design concepts such as TADF, exciplexes, and UENs to develop high-performance WOLEDs.

3.2.1. Early Explorations of UEN-Based WOLEDs

At the early stage, the working mechanism of UEN-based WOLEDs was still unclear. Hence, the performance of the devices was not satisfactory enough. However, the early efforts enabled the gradual development of UEN-based WOLEDs.

In 2013, Zhao et al. developed multiple combinations of complementary UEN-based WOLEDs [88]. The detailed device structures are shown in Figure 5, where (fbi)₂Ir(acac) is bis(2-(9,9-diethyl-9H-fluoren-2-yl)-1-phenyl-1H-benzimidazol-N,C3)iridium-(acetylacetonate), (ppy)₂Ir(acac) is bis(2-phenylpyridine)-(acetylacetonate)iridium(III), (piq)₂Ir(acac) is bis(1-phenyliso-quinoline)(acetylacetonate)iridium(III), and (MDQ)₂Ir(acac) is bis(2-methyldibenzo[f,h]-quinoxaline)(acetylacetonate) iridium(III). A thin TCTA interlayer was inserted into UENs to inhibit the energy transfer, and the luminescent color could be regulated by adjusting the thickness of the TCTA interlayer. The blue/orange, blue/green/red, and blue/green/orange/red WOLEDs showed the maximum EQEs of 16.4%, 18.5%, and 10.8%, respectively. Although four-color WOLEDs showed poorer performance in EQE, they had the highest CRI of 87. This study of UEN-based WOLEDs showed that UENs had great potential to develop undoped white devices. However, it also revealed there was a long way to go to achieve high performance. Subsequently, Zhu et al. inserted orange UENs into a blue emitter to fabricate WOLEDs [89]. The specific structure was ITO/MoO₃ (10 nm)/TAPC:MoO₃ (20%, 50 nm)/TAPC (30 nm)/TCTA: Flrpic (10%, 5 nm)/bis(2-phenyl-benzothiazolato-N,C^{2'})iridium-(acetylacetonate) [Ir(bt)₂(acac)] (0.02, 0.04, 0.06, 0.08 nm)/2,6-bis(3-(carbazol-9-yl)phenyl)pyridine (26DCzPPy): Flrpic (20%, 5 nm)/BmPyPB (10 nm)/BmPyPB:Li₂CO₃ (3%, 30 nm)/Li₂CO₃ (1 nm)/Al (100 nm), and the maximum PE, CE, and EQE reached 63.2 Lm/W, 59.3 cd/A, and 23.1%, respectively. The EL mechanism of the orange UENs was the energy transfer instead of the direct charge capture, and efficiency roll-off was caused by TTA.

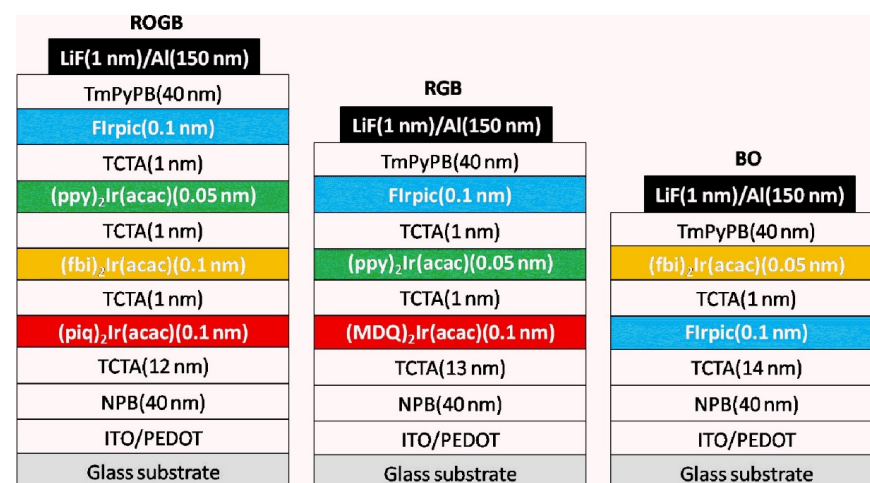


Figure 5. Device structure of WOLEDs based on doping-free UENs. Reproduced from reference [88], American Chemical Society, 2013 [88].

As hybrid WOLEDs may simultaneously achieve high efficiency and stability, Liu et al. utilized the structure of ITO/N,N,N',N'-tetrakis(4-methoxyphenyl)-benzidine (MeO-TPD): tetra-fluoro-tetracyanoqino dimethane (F4-TCNQ) (50 nm, 4%)/NPB (20 nm)/iridium(III) diazine complexes (MPPZ)2Ir(acac) (0.5 nm)/NPB (4 nm)/p-bis(p-N,N-di-phenyl-amino-styryl) benzene (DSA-ph) (0.2 nm)/TPBi (30 nm)/LiF (1 nm)/Al (200 nm) to fabricate WOLEDs with phosphorescent orange and fluorescent blue UENs [90]. It achieved the maximum CE and PE of 7.6 cd/A and 8.9 Lm/W, respectively, and the highest CRI was 75 in two-color hybrid WOLEDs based on an Ir complex. Also, Wang et al. developed hybrid WOLEDs with a PE of 9.93 Lm/W and EQE of 4.49% by using a blue UEN combined with a doped orange-emitting layer [91]. Zhao et al. developed a hybrid WOLED by using a yellow UEN combined with a doped blue light-emitting layer. However, the thin yellow-emitting layer resulted in lower efficiency due to electron leakage [92]. By properly thickening the yellow up to 1 nm, the CE of 79.0 cd/A and PE of 40.5 Lm/W were achieved. On the other hand, Jeon et al. combined the design concept of UENs and pre-mixing to develop WOLEDs based on pre-mixed UENs, and the color could be changed by adjusting the position of the UEN insertion and the pre-mixed composition [93]. Finally, white light of CIE (0.34, 0.34) and good color stability were achieved.

3.2.2. Further Developments of UEN-Based WOLEDs

As more insights about the working mechanisms of UEN-based WOLEDs have been uncovered, the huge potential of such WOLEDs has attracted great research attention worldwide. As a consequence, more and more strategically designed devices have been fabricated [94–99]. With the intensive endeavors taken by researchers, UEN-based WOLEDs achieved satisfactory performance compared to doped devices, further showing the advantages of the UEN-based technique.

Effects of Interlayers

By inserting an interlayer or spacer between UENs, the charge and exciton distribution may be manipulated accordingly, which is a feasible scheme to boost device performance. In general, interlayers can be unipolar or bipolar materials.

In 2015, Xue et al. put a lot of effort into improving high-performance UEN-based WOLEDs [60,63,100]. First, they fabricated WOLEDs with orange and blue UENs based on existing OLEDs with orange UENs. The detailed structure was ITO/MoO₃ (2 nm)/CBP [(70-Z) nm]/PO-01 (0.15 nm)/CBP (Z nm)/FIrPic (0.1 nm)/TPBi (30 nm)/LiF (0.8 nm)/Al (100 nm). The best CE and PE were 33.6 cd/A and 30.1 Lm/W, respectively, when Z was 4. In this case, they pointed out that the light emission layer could be regarded as a single layer with multi-doped dyes without differential color aging, resulting in outstanding spectra stability. As Z increased, Dexter energy transfer from FIrPic to PO-01 became less or was completely blocked, which meant that the charge recombination zone was moved and could be regarded as conventional WOLEDs with multiple emission layers. Then, they used CBP:TPBi instead of pure CBP as the interlayer to control the exciton distribution by changing the mixing ratio of CBP:TPBi so that the stability of white emitting was improved. They further developed three-color and four-color WOLEDs with UENs based on high-performance monochromatic OLEDs with UENs. The PE of three-color and four-color WOLEDs could reach 27.2 Lm/W and 26.0 Lm/W, respectively, and the devices realized lower turn-on voltage than conventional doping devices; e.g., for the PE of four-color UEN-based WOLEDs, there was a 39% improvement compared to doped devices. The reason for the high performance was that the energy barriers for charge injection at the interfaces in doped ones could be avoided, which led to the carriers accumulating at the narrow interfaces. In the same year, to achieve redistribution of excitons and more balanced white light emission, Tan et al. introduced TAPC as a hole trapping layer into WOLEDs based on UENs [101]; the detailed structure was ITO/PEDOT:PSS (25 nm)/TAPC (20 nm)/MCP (12 nm)/Red Dopant (0.2 nm)/MCP

(4 nm)/Flrpic (0.2 nm)/TAPC (0.8 nm)/TPBi (8 nm)/Ir(ppy)₃ (0.2 nm)/TPBi (32 nm)/LiF (1 nm)/Al (100 nm), and the CE and PE were 23.4 cd/A and 17.0 Lm/W, respectively.

In previous works, interlayers were demonstrated as one of the crucial factors for high device performance. So, more in-depth research on interlayers in UENs was conducted. Liu et al. further clarified the spacer's role and developed high-performance doping-free hybrid UEN-based WOLEDs, whose structure and materials are shown in Figure 6, where Ir(dmppy)₂(dpp) is bis(2-phenyl-4,5-dimethylpyridinato)[2-(biphenyl-3-yl)pyridinato] iridium(III) [102]. They thoroughly employed the doping-free principle; both UENs and other layers were doping-free. To achieve high performance, NPB and TPAC were combined as the HTL due to the high T₁ and LUMO of TPAC, which were 2.84 eV and 1.8 eV, respectively, confining the excitons and electrons. TmPyPB was selected as the ETL owing to its high electron mobility (10³ cm²/V s), deep HOMO of 6.7 eV, and high T₁ of 2.7 eV, which could effectively improve the electron injection, prevent the hole leakage, and confine the excitons. The authors first pointed out that the interlayers could avert the concentration quenching and unipolar interlayers were more conducive for doping-free hybrid WOLEDs than bipolar ones. After optimization, they obtained a device with a CRI of 91.3 and PE of 14.6 Lm/W.

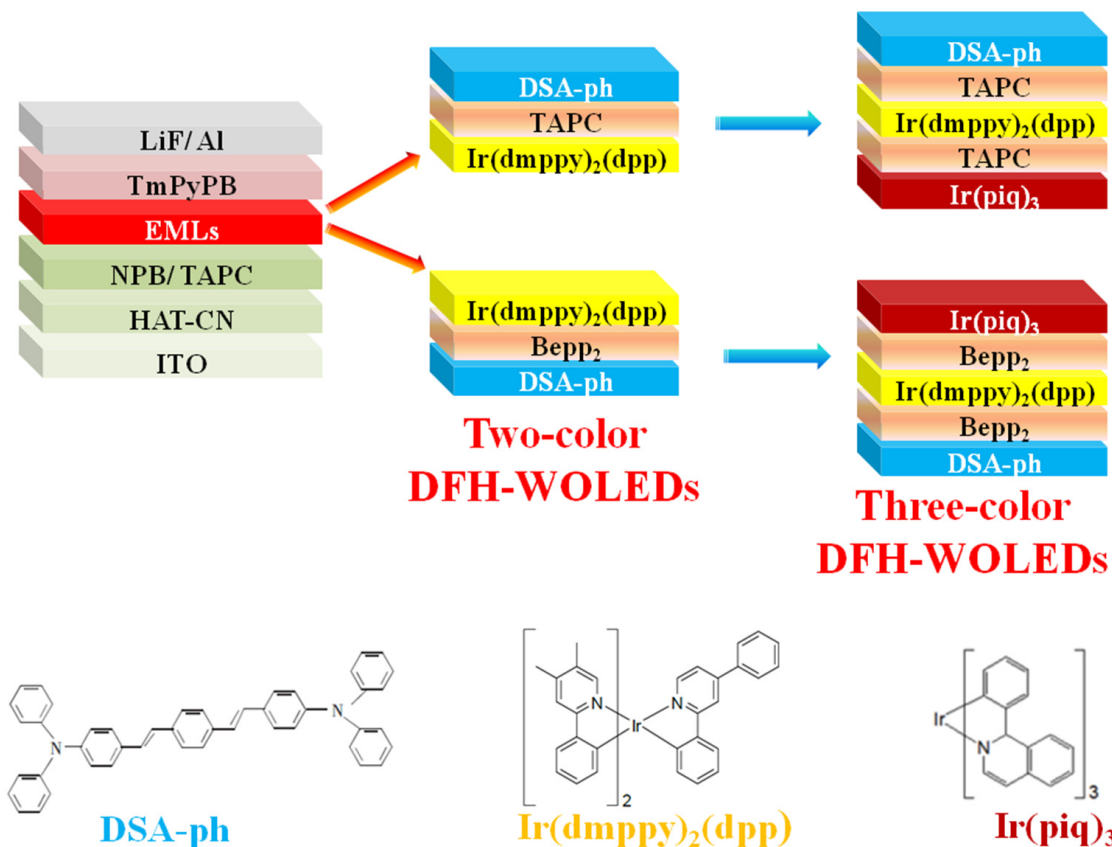


Figure 6. Schematic structures of the doping-free hybrid WOLEDs (DFH-WOLEDs) and the chemical structure of emitters. Reproduced from reference [102], Elsevier, 2016 [102].

To further promote the performance of UEN-based WOLEDs, bipolar emitting layers or interlayers were also strategically introduced to control the distribution of charges and excitons, where bipolar layers were generally the combination of p-type and n-type organic semiconductor materials with high energy states in order to guarantee the radiative recombination [103–107]. In 2018, Miao et al. used a bipolar N,N'-di-(1-naphthalenyl)-N,N'-diphenyl-[1,1':4',1'':4'',1''':4''',1''''-quaterphenyl]-4,4'''-diamine (4P-NPD)/4P-NPD: Bepp2 (1:1)/Bepp2 blue light-emitting layer; they first probed the mechanism of exciton utilization and energy transfer using two-color and three-color UEN-based WOLEDs

and finally developed red–yellow–green–blue four-color WOLEDs [108]. As a result, a maximum EQE of 21.46% and PE of 47.90 Lm/W were obtained with the device structure of ITO/MoO₃ (3 nm)/TAPC (40 nm)/Ir(piq)₂(acac) (0.1 nm)/4P-NPD (3 nm)/4P-NPD: Bepp2 (1:1, 3 nm)/bis(2-(3-trifluoromethyl-4-fluorophenyl)-4-methylquinolyl)-(acetylacetonate)-iridium(III) [Ir(ffpmq)₂(acac)] (0.06 nm)/4P-NPD: Bepp2 (1:1, 3 nm)/Bepp2 (3 nm)/Ir(ppy)₃ (0.2 nm)/TmPyPB (50 nm)/LiF (1 nm)/Al (100 nm). Also, Yu et al. deeply explored WOLEDs with UENs by using a TCTA and 1,3,5-tri(m-pyrid-3-yl-phenyl) benzene (TmPyPB) hybrid bipolar interlayer to achieve carrier balance and broaden the exciton distribution region to reduce triplet–polaron annihilation (TPA) and improve device lifetime [109]. The specific structure was ITO/MoO₃: TCTA (2:3, 35 nm)/TCTA (27-Z nm)/bis [2-(3,5-dimethylphenyl)-4-methyl-quinoline]-(acetylacetonate)-iridium(III) [Ir(mphmq)₂acac] (0.07 nm)/TCTA: Tm₃PyPB (3.5: 1, Z nm)/PO-01 (0.2 nm)/TCTA: Tm₃PyPB (3.5:1, 3 nm)/Ir(ppy)₂acac (0.15 nm)/TCTA: Tm₃PyPB (3.5:1, 3 nm)/FIRpic (0.1 nm)/Tm₃PyPB (40 nm)/LiF (1 nm)/Al (120 nm). The interlayer thickness could be adjusted, achieving emissions from short wavelength to long wavelength. Finally, they achieved a yellow–green–blue WOLED with a maximum CE of 47.8 cd/A and PE of 44.5 Lm/W. Dai et al. also made many efforts to develop high-performance three-color WOLEDs using the structure of ITO/MoO₃: TCTA (2:3, 35 nm)/TCTA (18 nm)/FIRpic (0.3 nm)/TCTA: TmPyPB (1:4 3 nm)/Ir(ppy)₂(acac) (0.15 nm)/TCTA: TmPyPB (1:4 3 nm)/PO-01 (0.05 nm)/TmPyPB (40 nm)/LiF (1 nm)/Al (100 nm), which achieved the CIE coordinate change of only (0.001, 0.001) when the luminance was varied from 1000 cd/m² to 10,000 cd/m², showing excellent color stability [110,111]. The peak CE, PE, and EQE in their work were 59.2 cd/A, 61.1 Lm/W, and 18.0%, respectively. The reasons for such excellent performance were as follows: the bipolar hybrid spacer TCTA: TmPyPB contributed to the uniform exciton distribution; the green UEN located in the middle mitigated the TTA and maintained the sequential energy transfer, which counteracted the emission intensity variation caused by the drift of exciton combination region at different voltages; and the carrier trapping effect was used to compensate for the emission intensity at low voltages.

In addition, UENs without interlayers were also developed. Wu et al. developed red–green–blue three-color and orange–blue two-color WOLEDs without the interlayer, achieving balanced white light emission by strategically adjusting the thickness of UENs with lower T₁ or singlet energy (S₁) for smooth exciton diffusion and sufficient energy transfer [112]. The structures of three-color and two-color WOLEDs were ITO/HAT-CN (10 nm)/TAPC (45 nm)/TCTA (10 nm)/Ir(MDQ)₂(acac) (0.02 nm)/Ir(ppy)₂(acac) (0.02 nm)/FIRpic (0.3 nm)/TmPyPB (40 nm)/Liq (2 nm)/Al (120 nm) and ITO/HAT-CN (10 nm)/TAPC (45 nm)/TCTA (10 nm)/PO-01 (0.02 nm)/FIRpic (0.3 nm)/TmPyPB (40 nm)/Liq (2 nm)/Al (120 nm). A PE of 55.5 lm/W was achieved, which was the highest efficiency at the time.

Position Optimization

To boost the efficiency of WOLEDs, the understanding of the position of UENs is significant, especially in multi-color WOLEDs, since the exciton recombination zone is affected by the charge dynamics [113–118].

Miao et al. conducted an in-depth study on multi-color WOLEDs based on UENs [31,119,120]. Firstly, the fluorescent blue light-emitting layer was inserted between the ETL and HTL, and the green and yellow light emitters doped in the ETL and HTL were controlled to keep them away from the interface between ETL/EML and HTL/EML. The red UENs were inserted in the blue emission layer to produce red–yellow–green–blue WOLEDs. The CE, PE, EQE, and CRI of the device reached 34.15 cd/A, 29.51 Lm/W, 17.71%, and 94, respectively. The researchers further inserted ultrathin red-, yellow-, and green-emitting layers into the blue light-emitting layer in a different order, and the specific structures of the devices and the best performance are shown in Figure 7. The final insertion resulted in a high EQE of 19.34% and an extremely superior CRI of 96. The high performance was mainly due to the precise control of the carrier recombination zone, allowing both singlet

and triplet excitons to be effectively utilized. Carrier recombination was confined to the entire EML and the interface between the EML and the adjacent layers, resulting in the fact that the generated singlet excitons could be directly recombined on Bepp₂ for blue emission, which also meant there was a prohibition of non-radiative decay loss related to transferring singlet excitons energy to ultrathin phosphorescent layers. Because of the longer diffusion distance for triplet excitons (>10 nm) and higher triplet level of Bepp₂ than those for phosphorescent emitters, the generated triplet excitons could diffuse to ultrathin phosphorescent layers and be used for phosphorescent emission. This ultimately allowed the generated excitons to be used efficiently, achieving 100% utilization in theory.

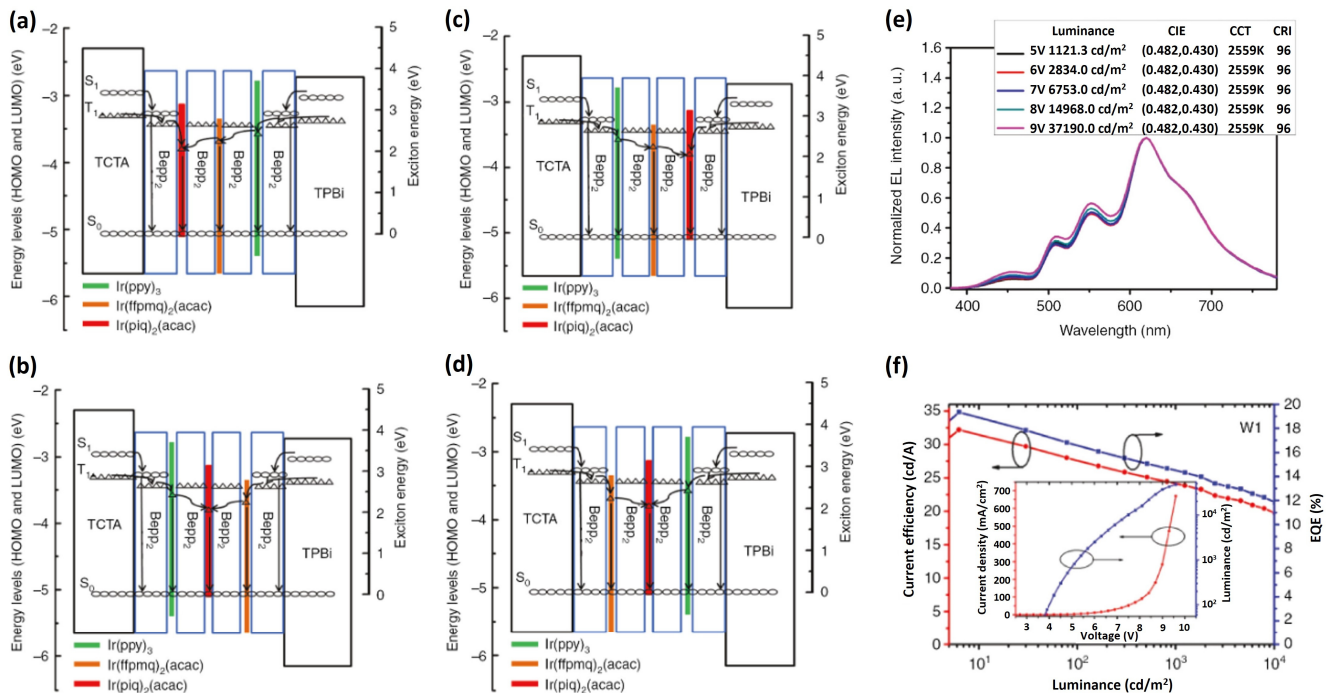


Figure 7. Schematic diagrams of the emission mechanisms of four white devices. (a) For device W1, (b) for device W2, (c) for device W3, (d) for device W4. The circles and triangles are the exciton energies (S_1 , S_0 , and T_1). The performance of the best device W1: (e) EL spectra, CIE coordinates, CCT, and CRI; (f) CE–L–EQE characteristic curves. Reproduced from reference [120], Walter de Gruyter, 2017 [120].

Additionally, Zhang et al. succeeded in increasing the exciton complex probability while suppressing annihilation by precisely tuning the positions of the three luminescent layers of red, green and blue, and they finally obtained the CE of 44.2 cd/A, PE of 39.0 Lm/W and EQE of 20.3% with the specific device structure of ITO (180 nm)/MoO₃ (10 nm)/MoO₃: TAPC (25%, 35 nm)/TAPC (12 nm)/TCTA (5 nm)/Ir(MDQ)2(acac) (0.05 nm)/TCTA (1 nm)/Flrpic (0.4 nm)/26DCzPPy (2 nm)/BmPyPB (2 nm)/Ir(ppy)2(acac) (0.2 nm)/BmPyPB (8 nm)/BmPyPB: Li₂CO₃ (3%, 25 nm)/Li₂CO₃ (1 nm)/Al (150 nm) [121]. Zhao et al. inserted an ultrathin bis (1-phenylisoquinoline) (acetylacetonate)iridium (III) [Ir(pq)2acac] red-emitting layer into the mSOAD blue-emitting layer to produce a red–blue two-color WOLED based on UENs and the best performance of the device obtained after an in-depth analysis of the number of UENs and position of the UEN insertion, obtaining the highest CE of 31.9 cd/A, PE of 30.4 Lm/W, and EQE of 17.3% [122].

Influence of Tandem Structures

The exploitation of tandem structures is a useful method for achieving high luminance, high efficiency, and a long lifetime [69,104,123]. Using tandem UEN-based WOLEDs could also achieve the mentioned advantages, but the use needs to be optimized.

Liu et al. applied the tandem design concept to DF-WOLEDs for the first time and fabricated yellow–blue and red–blue two-color tandem WOLEDs based on UENs, and the yellow–blue tandem device obtained the CE of 81.2 cd/A and the best luminance performance of 44,886 cd/m² among non-doped devices at that time [124]. Zhang et al. utilized a doping-free LiF/Al/HAT-CN structure as the charge generation unit (CGU) based on the UEN and tandem design concept [48]. In the CGU, dissociation of the complexes at the HAT-CN/NPB interface generated charge and utilized the Al/LiF layer to assist electron injection into the adjacent ETL. The device ultimately achieved an ultrahigh EQE and CE of 31.6% and 94.9 cd/A with the structure of ITO/PEDOT: PSS (40 nm)/EL unit/CGU/EL unit/LiF (1 nm)/Al (100 nm). The EL unit was NPB (30 nm)/TCTA (10 nm)/PO-01 (0.1 nm)/MCP (3 nm)/Firpic (0.25 nm)/TmPyPB (40 nm), where PO-01 and Firpic were used as non-doped blue and yellow UENs, respectively.

Introduction of Multi-Functional Emitting Materials

Similar to doped devices, the innovation of material engineering brings new space for the performance improvement of UEN-based WOLEDs [125]. Various multi-functional emitting materials have been introduced to construct UEN-based WOLEDs, such as aggregation-induced emission (AIE) materials, exciplex materials, and TADF materials. With the understanding of the chemistry and physics of multi-functional emitting materials, high device performance has been yielded.

Firstly, avoiding the aggregation-caused quenching issue is challenging for developing high-performance UEN-based WOLEDs, particularly for blue fluorophores. Unlike conventional chromophores, AIE luminogens can overcome the quenching problem caused by aggregation, since aggregation can improve rather than quench their emissions. Therefore, AIEgens are promising for DF-OLEDs avoiding thickness restriction. Liu et al. introduced an AIE material, blue BTPEAn, into DF-WOLEDs for the first time and used it as a UEN to fabricate WOLEDs, which exhibited high device performance (e.g., pure-white colors, high efficiency, or sunlight-like emissions) [126]. The architecture of the three-color devices was ITO/HAT-CN (100 nm)/NPB (15 nm)/TAPC (5 nm)/Ir(piq)₃ (0.3 nm)/TAPC (1.5 nm)/Ir(dmppy)₂(dpp) (0.9 nm)/TAPC (3.5 nm)/BTPEAn (0.4, or 15 nm) 1,3,5-tri(m-pyrid-3-yl-phenyl)benzene (TmPyPB, 35 nm)/Cs₂CO₃ (1 nm)/Al (160 nm), and the CRI of 92.8 reached a new record among OLEDs based on AIE materials at that time.

Additionally, the introduction of exciplex materials has recently been found to be effective in developing high-performance UEN-based WOLEDs. Zhang et al. conducted extensive and in-depth research on this and developed high-performance UEN-based WOLEDs by arranging red, green, and blue UENs in an mCBP: PO-T2T exciplex in different sequences [78]. The best-performing device had the EQE of 26.1%, CE of 40.0 cd/A, PE of 50.1 Lm/W, and CRI of 81 with the structure of ITO/HAT-CN (15 nm)/TAPC (50 nm)/TCTA (5 nm)/mCBP (3 nm)/Flrpic (0.05 nm)/mCBP (2 nm)/mCBP: PO-T2T (1:1, 2 nm)/Flrpic(0.2 nm)/mCBP: PO-T2T (1:1, 2 nm)/Ir(ppy)₂acac (0.1 nm)/mCBP: PO-T2T (1:1, 2 nm)/RD071 (red emitter, 0.05 nm)/mCBP: PO-T2T (1:1, 2 nm)/Flrpic (0.1 nm)/PO-T2T (40 nm)/LiF (1 nm)/Al. Compared to the previous devices, the blue light-emitting ratio was increased, which meant that more excitons of mCBP: PO-T2T were utilized due to the inserted Flrpic UENs with a precise thickness design, resulting in the fact that correlated color temperature (CCT) was increased to 2827 K while CRI stayed above 80. Furthermore, the WOLEDs achieved a barrier-free structure between HTL/ETL and UENs to efficiently inject carriers due to a reasonable arrangement of energy levels.

Also, Ying et al. inserted orange UENs into a blue mCBP: PO-T2T exciplex to obtain high performance [127]. The EQE and PE of the best-performance device could reach 22.45% and 97.1 Lm/W, respectively. The specific structure was ITO/HAT-CN (15 nm)/TAPC (50 nm)/TCTA (5 nm)/mCBP (5 nm)/mCBP: PO-T2T (1:1, 25 nm)/PO-T2T (45 nm)/Liq (1.5 nm)/Al (150 nm), in which the inserted iridium(III)bis(4-(4-t-butylphenyl)thieno-[3,2-c]pyridinato-N,C₂)acetylacetonate [Ir(tp₂tpy)₂acac] could be intelligently energy aligned with the mCBP: PO-T2T exciplex, which contributed to effective confinement of excitons

and the barrier-free carrier injection. The authors pointed out that the emission was mainly due to the efficient energy transfer from the exciplex to the UENs, and changing the locations of UENs would not essentially affect the performance of hybrid WOLEDs. Chen et al. also utilized a mCBP: PO-T2T exciplex to design UEN-based WOLEDs [128]. They used materials and structures similar to those used by Zhang [78]. The difference was that they used mCBP: PO-T2T as a blue emitter rather than FIrpic. The peak EQE, CE, PE, and CRI were 21.9%, 52.1 cd/A, 67.1 Lm/W, and 85, respectively. Zhao et al. also inserted multiple yellow UENs into a blue exciplex to produce yellow–blue WOLEDs with the optimized structure of ITO (180 nm)/MoO₃ (8 nm)/TCTA: MoO₃ (15%, 50 nm)/TCTA (10 nm)/4,40-bis(9-carbazolyl)-2,20-dimethylbiphenyl (CDBP) (10 nm)/CDBP: PO-T2T (7.5 nm)/PO-01 (0.02 nm)/CDBP: PO-T2T (2.5 nm)/PO-01 (0.02 nm)/(2.5 nm)/PO-01 (0.02 nm)/CDBP: PO-T2T (7.5 nm)/PO-T2T (10 nm)/PO-T2T: Li₂CO₃ (3%, 45 nm)/Li₂CO₃ (1 nm)/Al, which achieved high performance with the CE, PE, and EQE of 62.8 cd/A, 75.9 Lm/W, and 20.4%, respectively [129]. In addition, MCP: PO-T2T [130] and mCBP: PO-T2T [131] were also demonstrated to be excellent exciplex emitters, which could work well with complementary-color UENs to furnish white emissions.

On the other hand, TADF materials have been demonstrated to be effective for improving device performance because of their ability to harvest singlet and triplet excitons [123,132,133]. Liao et al. first used the blue TADF material 10, 10,10-(4,4,4-Phosphoryltris(benzene-4,1-diyl))tris-(10Hphenoxazine) (TPXZPO) as the n-type interlayer switch for the structure of ITO/HAT-CN (10 nm)/TAPC (40 nm)/MCP (15-x nm)/bis(2-benzothiophen-2-ylpyridine) (acetylacetonate) iridium (III) [Ir(bt)2acac] (0.5 nm)/TPXZPO (x = 1, 2, 3, 5, 10 nm)/Firpic (0.5 nm)/4,6-bis(3,5-di(pyridin-4-yl)phenyl)-2-phenylpyrimidine (B4Py-PPM) (40 nm)/LiF(0.8 nm)/Al (150 nm) [134]. In the best performance, the CE of 38.93 cd/A, PE of 37.05 Lm/W, and EQE of 14.96% could be reached. The excitons generated in TPXZPO were completely transferred to Ir(bt)2acac, while the interlayer played a key role in regulating exciton and charge distribution. Zhao et al. utilized the blue TADF material DMAC-DPS to develop UEN-based WOLEDs and fabricated yellow–blue WOLEDs with the CE, PE, and EQE of 34.9 cd/A, 29.2 Lm/W, and 11.4%, respectively [135]. Xue et al. obtained good EQE and CRI of 18.7% and 88, respectively, with only about 7% efficiency roll-off, by inserting red and yellow UENs into the bluish-green TADF material 10-[4-(4,6-diphenyl-1,3,5-triazin-2-yl)phenyl]-9,9-dimethylacridan (DMAC-TRZ) [136]. The detailed structure was ITO/HAT-CN (10 nm)/TAPC (50 nm)/TCTA (10 nm)/DMAC-TRZ (6 nm)/PO-01 (0.8 nm)/DMAC-TRZ (3 nm)/Ir(piq)3 (0.2 nm)/DMAC-TRZ (3 nm)/PO-01 (0.8 nm)/DMAC-TRZ (6 nm)/4,6-bis(3,5-di(pyridin-3-yl)phenyl)-2-(pyridin-3-yl) pyrimidine (B3PYMPM) (50 nm)/Liq (1 nm)/Al (120 nm). The WOLEDs used materials with a high T1 energy level, TCTA and B3PYMPM, to confine excitons, while TTA could be suppressed due to the insertion of several bipolar UENs contributing to improving exciton utilization and expanding exciton distribution. In 2022, Zhang et al. applied the TADF material 9,10-bis(4-(9H-carbazol-9-yl)-2,6-dimethylphenyl)-9,10-diboraanthracene (CzDBA) as UENs in WOLEDs and could achieve the maximum EQE of about 8% [137]. They analyzed densities of excitons at a steady state and pointed out that the non-radiative decay of triplets might reduce the EQE. Therefore, TADF materials could be effective in improving performance owing to the lower triplet-to-singlet energy gap and faster singlet radiative recombination rate.

Meanwhile, exciplexes with TADF properties are also beneficial for guaranteeing the high performance of UMN-based WOLEDs. For instance, Sheng et al. developed WOLEDs based on the combination of materials with TADF and exciplex properties to develop high-performance WOLEDs with the structure of ITO/HAT-CN (10 nm)/TAPC (40 nm)/TCTA (5 nm)/26DCzPPy (5 nm)/PO-01 (0.1 nm)/26DCzPPy (3 nm)/PO-T2T:6% 10-(4-(4,6-diphenyl-1,3,5-triazin-2-yl)phenyl)-10H-spiro[acridine-9,9'-fluorene] (SpiroAC-TRZ) (15 nm)/PO-T2T (30 nm)/Liq (1 nm)/Al, achieving a high PE of 60.9 Lm/W and good color stability [138]. Sun et al. fabricated two-color WOLEDs by inserting red UENs into the bluish-green TADF material DMAC-TRZ, which could harvest superfluous triplet

excitons within emitters and reduce quenching caused by local exciton accumulation [139]. In addition, the strong hole traps of UENs resulted in the improvement of carrier balance, which brought about a stable recombination zone. Finally, they developed excellent-performance UEN-based WOLEDs, as shown in Figure 8, achieving low efficiency roll-off and excellent color stability with the CE, PE, and EQE of 63.84 cd/A, 66.06 Lm/W, and 28.16%, respectively.

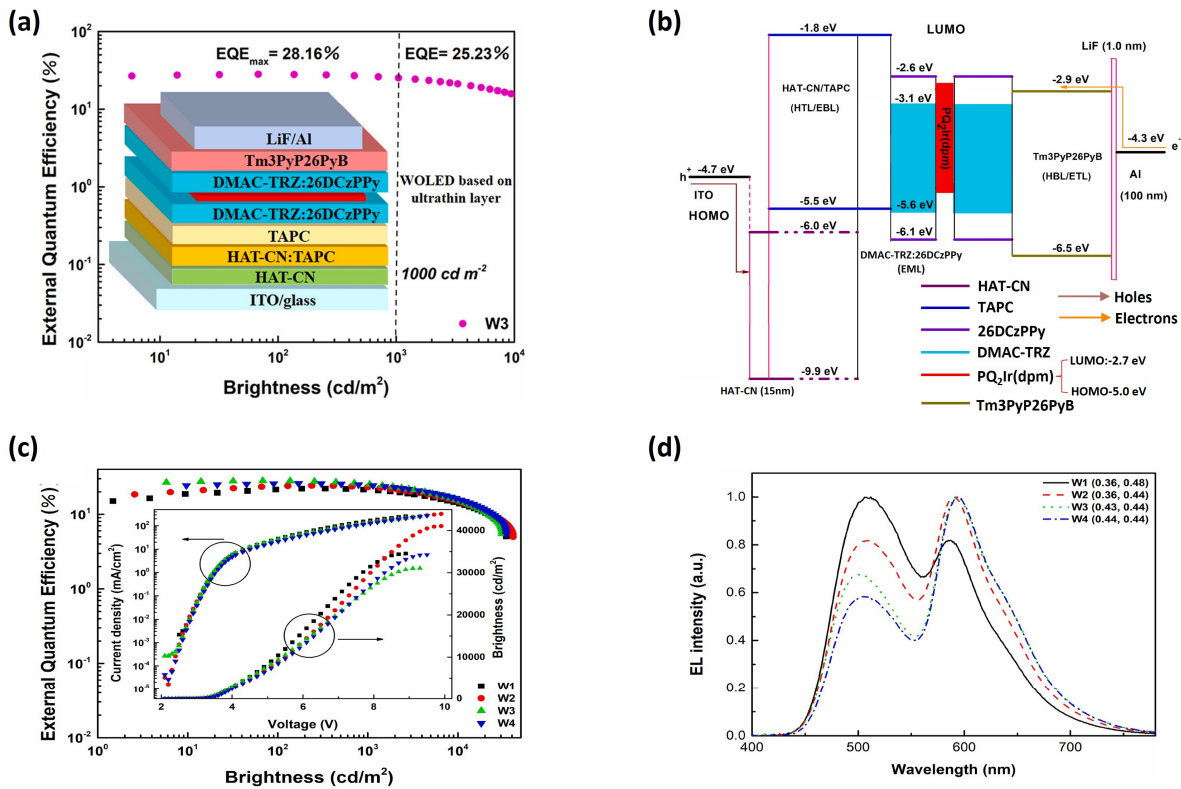


Figure 8. (a) Graphical abstract of the work. (b) Proposed energy-level diagram of hybrid warm WOLEDs. (c) External quantum efficiency–brightness characteristics of devices W1, W2, W3, and W4. Inset: Current density–brightness–voltage (J–B–V) characteristics of devices W1, W2, W3, and W4. (d) Normalized EL spectra of devices W1, W2, W3, and W4 operating at 10 mA/cm². Reproduced from reference [139], Elsevier, 2022 [139].

Table 1. Performance summary of representative UEN-based OLEDs in recent years.

Devices	EQE (%)	CE (cd/A)	PE (Lm/W)	CRI	Luminance (cd/m²)	CIE	Ref.
Red	20.90	38.48	44.78	--	14,410	(0.589,0.369)	[80]
Orange/yellow	22.8	52.0	65.3	--	20,800	--	[62]
	24.5	57.87	78.95	--	20,890	(0.510,0.481)	[80]
Green	25.5	98.0	85.4	--	--	--	[66]
	23.8	~60	~80	--	--	--	[72]
Blue	30.21	59.34	74.55	--	8578	(0.162,0.367)	[80]
	27.4	48.3	57.1	--	--	--	[78]
	22.45	74.2	97.1	--	--	--	[127]
White	28.16	63.84	66.06	78	31,094	(0.43,0.44)	[139]
	21.9	52.1	67.1	85	--	(0.38,0.46)	[128]
	26.1	40.0	50.1	81	--	(0.459,0.426)	[78]
	22.70	58.58	76.70	66	25,400	(0.426,0.491)	[80]
	23.88	56.41	70.89	75	16,110	(0.437,0.424)	[80]
	19.34	32.19	30.65	96	47,470	(0.482,0.430)	[31]

3.2.3. Degradation Mechanisms of UEN-Based OLEDs

In general, the reliability of UEN-based OLEDs is rarely reported, which may be attributed to the fact that the device lifetime is still far from satisfactory. The poor stability originates from both the used materials and device structures [140–144]. On one hand, the emitting materials greatly decide the lifetime of OLED devices [145–150]. In particular, since there is no stable blue phosphorescence or TADF blue-emitting materials so far, achieving UEN-based OLEDs with a long lifetime is a great challenge. In addition, charge-transporting materials play a significant role in device degradation [151–154]. For example, inorganic charge-transporting materials usually exhibit better stability than their organic counterparts. The stability is even different for organic materials (e.g., TCTA is more stable than TAPC and CBP). On the other hand, the device engineering also affects the stability of UEN-based OLEDs, since charge and exciton dynamics have an important influence on emission performance (e.g., charge–exciton interaction, exciton recombination and quenching) [155–161]. Additionally, although almost no attention has been paid to the optical effect of UEN-based OLEDs, this effect is significant for device lifetime since excess thermal energy is generated by the trapped light [162–169].

Similar to conventional OLEDs, UEN-based OLEDs also suffer from water and oxygen attack, electrochemical and photochemical reactions, electrical and thermal breakdown, etc. [170–174]. However, compared to conventional devices, UEN-based OLEDs may be more influenced by electron-induced molecule migration. The molecules of UENs are scattered in islands on the rough adjacent layers, showing a two-dimensional doping effect. However, the delicate design is more easily affected when making the EML thinner. The molecule migration induced by the flow and collision of electrons can easily destroy this two-dimensional doping form and causes the molecular distribution of the EML to become scattered in a way that was not anticipated at the time of design. At the time of design time, there may be a need for strategies to improve device performance such as confining the excitons and electrons [175–180].

4. Conclusions and Outlook

As UENs would simplify device structures, minimize fabrication procedures, and reduce the cost, a great number of UEN-based monochromatic and white OLEDs have been reported in recent years. Nowadays, the performance of OLEDs with UENs can be somewhat comparable to that of the state-of-the-art doping counterparts. Herein, we have reviewed the recent progress in the field of UEN-based OLEDs. Specifically, we have emphasized some representative high-performance UEN-based red, yellow/orange, green, blue, and white OLEDs.

Research on UEN-based OLEDs started from monochromatic colors and extended to white emissions. Afterward, the emission mechanism of UEN-based OLEDs was explored. It was found that UENs directly captured very few charges, while the dominant mechanism of device luminescence was usually the energy transfer between the host and the guest. With a greater understanding of emission mechanisms, researchers gradually applied new materials and design concepts (e.g., interlayer, AIE, exciplex, and TADF materials) to the development of UEN-based WOLEDs. Although the performance of UEN-based OLEDs has been gradually enhanced, there are still many challenges limiting their practical applications, such as efficiency, efficiency roll-off, and lifetime. In the case of efficiency, as the EQE is decided by the outcoupling factor, the fraction of excitons decayed radiatively, the photoluminescence quantum efficiency of emitters, and charge balance, the material and device engineering should be well controlled [181–185]. Additionally, since PE is inversely proportional to operational voltages, future works also need to focus on how to reduce the voltages in order to achieve the theoretical PE limit of WOLEDs (248 Lm/W) [55,186–189]. To lower the efficiency roll-off, charge balance is typically required. Hence, the selection of charge transport layers, the design of interlayers, and the position of UENs should be carefully managed [6,190–192].

In terms of device lifetime, it is worth noting that UEN-based OLEDs have not yet obtained satisfactory stability, even for monochromatic green OLEDs. Therefore, there is still a large gap between UEN-based OLEDs and advanced doped OLEDs from the perspective of stability [193]. As the lifetime is a crucial factor determining the commercial potential of products, more efforts are necessary to be made to enhance the stability of UEN-based OLEDs. In particular, the stability mechanism of UEN-based OLEDs is still unclear, requiring an insightful understanding of charge and exciton behaviors [194–197]. In particular, by virtue of inorganic charge transport materials, the device stability may be improved, although almost no such work has been reported [198–201]. In addition, due to the high exciton utilization efficiency of TADF emitters, more and more researchers have adopted TADF materials for UENs in order to develop high-performance OLEDs. However, there is still a lack of stable TADF materials that can efficiently produce deep blue emissions, which is an important limiting factor for UEN-based blue and white OLEDs. Hence, the innovation of device structures may be helpful (e.g., the use of tandem structures, the design of warm-white emissions). Once the above issues are solved, UEN-based OLEDs are believed to have bright prospects for mass production and play an important role in the display and lighting fields.

Author Contributions: B.L. and Y.Z. conceived the idea; Y.Z., H.G. and B.L. wrote the paper, D.L., J.W., F.S.Y.Y., S.L. (Shenghuang Lin) and X.L. advised the paper; B.L., H.S.K., D.L. and S.L. (Shaolin Liao) supervised the project. All authors have read and agreed to the published version of the manuscript.

Funding: This work was supported by the Guangdong Innovation and Entrepreneurship Team Project under Grant 2021ZT09X070, National Natural Science Foundation of China under Grant 62104265, Guangdong Science and Technology Plan under Grant 2022A0505020022, Science and Technology Program of Guangdong Province under Grant 2021A0505110009, the Innovation and Technology Fund under Grant GHP/006/20GD, the Fundamental and Applied Basic Research Project of Guangzhou City under Grant 202201011534, and Fundamental Research Funds for the Central Universities, Sun Yat-sen University (23qnp25). Shaolin Liao is partially supported by related projects of Guangdong Zhujiang Leadership Project under Grant 2021CX02X011, Chinese Ministry of Science and Technology's Huoju Talent Project under Grant 2023HJJH01.

Data Availability Statement: Data available in a publicly accessible repository.

Conflicts of Interest: The authors declare no conflict of interest.

References

1. Tang, C.W.; VanSlyke, S.A. Organic electroluminescent diodes. *Appl. Phys. Lett.* **1987**, *51*, 913–915. [[CrossRef](#)]
2. Baldo, A.; O'Brien, D.; You, Y.; Shoustikov, A.; Sibley, S.; Thompson, M.E.; Forrest, S.R. Highly efficient phosphorescent emission from organic electroluminescent devices. *Nature* **1998**, *395*, 151–154. [[CrossRef](#)]
3. Reineke, S.; Lindner, F.; Schwartz, G.; Seidler, N.; Walzer, K.; Lussem, B.; Leo, K. White organic light-emitting diodes with fluorescent tube efficiency. *Nature* **2009**, *459*, 234–238. [[CrossRef](#)]
4. So, F.; Kido, J.; Burrows, P. Organic Light-Emitting Devices for Solid-State Lighting. *MRS Bull.* **2008**, *33*, 663–669. [[CrossRef](#)]
5. Su, S.J.; Gonmori, E.; Sasabe, H.; Kido, J. Highly Efficient Organic Blue-and White-Light-Emitting Devices Having a Carrier- and Exciton-Confining Structure for Reduced Efficiency Roll-Off. *Adv. Mater.* **2008**, *20*, 4189–4194. [[CrossRef](#)]
6. Wang, Z.B.; Helander, M.G.; Qiu, J.; Puzzo, D.P.; Greiner, M.T.; Hudson, Z.M.; Wang, S.; Liu, Z.W.; Lu, Z.H. Unlocking the full potential of organic light-emitting diodes on flexible plastic. *Nat. Photonics* **2011**, *5*, 753–757. [[CrossRef](#)]
7. Goushi, K.; Yoshida, K.; Sato, K.; Adachi, C. Organic light-emitting diodes employing efficient intersystem crossing for triplet-to-singlet state conversion. *Nat. Photonics* **2012**, *6*, 253–258. [[CrossRef](#)]
8. Liu, B.; Luo, D.; Gao, D.; Wang, X.; Xu, M.; Zou, J.; Ning, H.; Wang, L.; Peng, J.; Cao, Y. An ideal host-guest system to accomplish high-performance greenish yellow and hybrid white organic light-emitting diodes. *Org. Electron.* **2015**, *27*, 29–34. [[CrossRef](#)]
9. Wu, Z.; Liu, Y.; Yu, L.; Zhao, C.; Yang, D.; Qiao, X.; Chen, J.; Yang, C.; Kleemann, H.; Leo, K.; et al. Strategic-tuning of radiative excitons for efficient and stable fluorescent white organic light-emitting diodes. *Nat. Commun.* **2019**, *10*, 2380. [[CrossRef](#)] [[PubMed](#)]
10. Luo, D.; Li, X.L.; Zhao, Y.; Gao, Y.; Liu, B. High-Performance Blue Molecular Emitter-Free and Doping-Free Hybrid White Organic Light-Emitting Diodes: An Alternative Concept To Manipulate Charges and Excitons Based on Exciplex and Electroplex Emission. *ACS Photonics* **2017**, *4*, 1566–1575. [[CrossRef](#)]
11. D'Andrade, B.W.; Holmes, R.J.; Forrest, S.R. Efficient Organic Electrophosphorescent White-Light-Emitting Device with a Triple Doped Emissive Layer. *Adv. Mater.* **2004**, *16*, 624–628. [[CrossRef](#)]

12. Lee, Y.H.; Lee, W.; Lee, T.; Jung, J.; Yoo, S.; Lee, M.H. Achieving over 36% EQE in blue OLEDs using rigid TADF emitters based on spiro-donor and spiro-B-heterotriangulene acceptors. *Chem. Eng. J.* **2023**, *452*, 139387. [[CrossRef](#)]
13. Afzal, Z.; Hussain, R.; Khan, M.U.; Khalid, M.; Iqbal, J.; Alvi, M.U.; Adnan, M.; Ahmed, M.; Mehboob, M.Y.; Hussain, M.; et al. Designing indenothiophene-based acceptor materials with efficient photovoltaic parameters for fullerene-free organic solar cells. *J. Mol. Model.* **2020**, *26*, 137. [[CrossRef](#)] [[PubMed](#)]
14. Mahmood, A.; Sandali, Y.; Wang, J.L. Easy and fast prediction of green solvents for small molecule donor-based organic solar cells through machine learning. *Phys. Chem. Chem. Phys.* **2023**, *25*, 10417–10426. [[CrossRef](#)] [[PubMed](#)]
15. Hussain, R.; Khan, M.U.; Mehboob, M.Y.; Khalid, M.; Iqbal, J.; Ayub, K.; Adnan, M.; Ahmed, M.; Atiq, K.; Mahmood, K. Enhancement in Photovoltaic Properties of N,N-diethylaniline based Donor Materials by Bridging Core Modifications for Efficient Solar Cells. *ChemistrySelect* **2020**, *5*, 5022–5034. [[CrossRef](#)]
16. Mehboob, M.Y.; Hussain, R.; Khan, M.U.; Adnan, M.; Umar, A.; Alvi, M.U.; Ahmed, M.; Khalid, M.; Iqbal, J.; Akhtar, M.N.; et al. Designing N-phenylaniline-triazol configured donor materials with promising optoelectronic properties for high-efficiency solar cells. *Comput. Theor. Chem.* **2022**, *1186*, 112908. [[CrossRef](#)]
17. Cho, Y.J.; Yook, K.S.; Lee, J.Y. Cool and warm hybrid white organic light-emitting diode with blue delayed fluorescent emitter both as blue emitter and triplet host. *Sci. Rep.* **2015**, *5*, 7859. [[CrossRef](#)]
18. Kim, B.S.; Yook, K.S.; Lee, J.Y. Above 20% external quantum efficiency in novel hybrid white organic light-emitting diodes having green thermally activated delayed fluorescent emitter. *Sci. Rep.* **2014**, *4*, 6019. [[CrossRef](#)]
19. Xiao, P.; Huang, J.; Yan, D.; Luo, D.; Yuan, J.; Liu, B.; Liang, D. Emergence of Nanoplatelet Light-Emitting Diodes. *Materials* **2018**, *11*, 1376. [[CrossRef](#)]
20. Xiao, P.; Yu, Y.; Cheng, J.; Chen, Y.; Yuan, S.; Chen, J.; Yuan, J.; Liu, B. Advances in Perovskite Light-Emitting Diodes Possessing Improved Lifetime. *Nanomaterials* **2021**, *11*, 103. [[CrossRef](#)]
21. Luo, D.; Chen, Q.; Qiu, Y.; Zhang, M.; Liu, B. Device Engineering for All-Inorganic Perovskite Light-Emitting Diodes. *Nanomaterials* **2019**, *9*, 1007. [[CrossRef](#)]
22. Liu, B.; Li, X.L.; Tao, H.; Zou, J.; Xu, M.; Wang, L.; Peng, J.; Cao, Y. Manipulation of exciton distribution for high-performance fluorescent/phosphorescent hybrid white organic light-emitting diodes. *J. Mater. Chem. C* **2017**, *5*, 7668–7683. [[CrossRef](#)]
23. Liu, B.; Wang, L.; Zou, J.; Tao, H.; Su, Y.; Gao, D.; Xu, M.; Lan, L.; Peng, J. Investigation on spacers and structures: A simple but effective approach toward high-performance hybrid white organic light emitting diodes. *Synth. Met.* **2013**, *184*, 5–9. [[CrossRef](#)]
24. Luo, D.; Xiao, P.; Liu, B. Doping-Free White Organic Light-Emitting Diodes. *Chem. Rec.* **2019**, *19*, 1596–1610. [[CrossRef](#)] [[PubMed](#)]
25. Luo, D.; Chen, Q.; Gao, Y.; Zhang, M.; Liu, B. Extremely Simplified, High-Performance, and Doping-Free White Organic Light-Emitting Diodes Based on a Single Thermally Activated Delayed Fluorescent Emitter. *ACS Energy Lett.* **2018**, *3*, 1531–1538. [[CrossRef](#)]
26. Luo, D.; Xiao, Y.; Hao, M.; Zhao, Y.; Yang, Y.; Gao, Y.; Liu, B. Doping-free white organic light-emitting diodes without blue molecular emitter: An unexplored approach to achieve high performance via exciplex emission. *Appl. Phys. Lett.* **2017**, *110*, 061105. [[CrossRef](#)]
27. Han, H.; Hu, S.; Zhang, S.; Li, X.; Sun, H.; Chen, J.; Liu, B.; Liu, C.; Chen, W.; Zhang, Q. Achieving Solution-Processed Non-Doped Single-Emitting-Layer White Organic Light-Emitting Diodes through Adjusting Pyrene-Based Polyaromatic Hydrocarbon. *Chemistry* **2022**, *28*, e202201741.
28. Miao, Y.; Yin, M. Recent progress on organic light-emitting diodes with phosphorescent ultrathin (<1 nm) light-emitting layers. *iScience* **2022**, *25*, 103804.
29. Zhao, Y.; Chen, J.; Ma, D. Realization of high efficiency orange and white organic light emitting diodes by introducing an ultra-thin undoped orange emitting layer. *Appl. Phys. Lett.* **2011**, *99*, 163303. [[CrossRef](#)]
30. Liu, B.; Hu, S.; Zhang, L.; Xiao, P.; Huang, L.; Liu, C. Blue Molecular Emitter-Free and Doping-Free White Organic Light-Emitting Diodes With High Color Rendering. *IEEE Electron Device Lett.* **2021**, *42*, 387–390. [[CrossRef](#)]
31. Miao, Y.; Wang, K.; Zhao, B.; Gao, L.; Wang, Y.; Wang, H.; Xu, B.; Zhu, F. Manipulation and exploitation of singlet and triplet excitons for hybrid white organic light-emitting diodes with superior efficiency/CRI/color stability. *J. Mater. Chem. C* **2017**, *5*, 12474–12482. [[CrossRef](#)]
32. Zhang, L.; Li, X.L.; Luo, D.; Xiao, P.; Xiao, W.; Song, Y.; Ang, Q.; Liu, B. Strategies to Achieve High-Performance White Organic Light-Emitting Diodes. *Materials* **2017**, *10*, 1378. [[CrossRef](#)]
33. Luo, D.; Yang, Y.; Huang, L.; Liu, B.; Zhao, Y. High-performance hybrid white organic light-emitting diodes exploiting blue thermally activated delayed fluorescent dyes. *Dyes Pigm.* **2017**, *147*, 83–89. [[CrossRef](#)]
34. Xiao, P.; Dong, T.; Xie, J.; Luo, D.; Yuan, J.; Liu, B. Emergence of White Organic Light-Emitting Diodes Based on Thermally Activated Delayed Fluorescence. *Appl. Sci.* **2018**, *8*, 299. [[CrossRef](#)]
35. Liu, B.; Gao, D.; Wang, J.; Wang, X.; Wang, L.; Zou, J.; Ning, H.; Peng, J. Progress of White Organic Light-Emitting Diodes. *Acta Phys. Chim. Sin.* **2015**, *31*, 1823–1852.
36. Liu, B.; Zou, J.; Su, Y.; Gao, D.; Lan, L.; Tao, H.; Peng, J. Hybrid white organic light emitting diodes with low efficiency roll-off, stable color and extreme brightness. *J. Lumin.* **2014**, *151*, 161–164. [[CrossRef](#)]
37. Sun, Y.; Giebink, N.C.; Kanno, H.; Ma, B.; Thompson, M.E.; Forrest, S.R. Management of singlet and triplet excitons for efficient white organic light-emitting devices. *Nature* **2006**, *440*, 908–912. [[CrossRef](#)] [[PubMed](#)]

38. Liu, B.; Xu, M.; Wang, L.; Zou, J.; Tao, H.; Su, Y.; Gao, D.; Ning, H.; Lan, L.; Peng, J. Regulating charges and excitons in simplified hybrid white organic light-emitting diodes: The key role of concentration in single dopant host–guest systems. *Org. Electron.* **2014**, *15*, 2616–2623. [[CrossRef](#)]
39. Jeon, S.O.; Lee, K.H.; Kim, J.S.; Ihn, S.G.; Chung, Y.S.; Kim, J.W.; Lee, H.; Kim, S.; Choi, H.; Lee, J.Y. High-efficiency, long-lifetime deep-blue organic light-emitting diodes. *Nat. Photonics* **2021**, *15*, 208–215. [[CrossRef](#)]
40. Sun, J.; Ahn, H.; Kang, S.; Ko, S.B.; Song, D.; Um, H.A.; Kim, S.; Lee, Y.; Jeon, P.; Hwang, S.H.; et al. Exceptionally stable blue phosphorescent organic light-emitting diodes. *Nat. Photonics* **2022**, *16*, 212–218. [[CrossRef](#)]
41. Baek, S.Y.; Kwak, S.Y.; Kim, S.T.; Hwang, K.Y.; Koo, H.; Son, W.J.; Choi, B.; Kim, S.; Choi, H.; Baik, M.H. Ancillary ligand increases the efficiency of heteroleptic Ir-based triplet emitters in OLED devices. *Nat. Commun.* **2020**, *11*, 2292. [[CrossRef](#)] [[PubMed](#)]
42. Park, Y.; Lee, G.S.; Lee, W.; Yoo, S.; Kim, Y.H.; Choi, K.C. Heteroleptic Ir(III)-based near-infrared organic light-emitting diodes with high radiance capacity. *Sci. Rep.* **2023**, *13*, 1369. [[CrossRef](#)]
43. Cheng, T.Y.; Lee, J.H.; Chen, C.H.; Chen, P.H.; Wang, P.S.; Lin, C.E.; Lin, B.Y.; Lan, Y.H.; Hsieh, Y.H.; Huang, J.J.; et al. Carrier Transport and Recombination Mechanism in Blue Phosphorescent Organic Light-Emitting Diode with Hosts Consisting of Cabazole- and Triazole-Moiety. *Sci. Rep.* **2019**, *9*, 3654. [[CrossRef](#)] [[PubMed](#)]
44. Liu, B.; Xu, M.; Wang, L.; Tao, H.; Su, Y.; Gao, D.; Lan, L.; Zou, J.; Peng, J. Simplified hybrid white organic light-emitting diodes with efficiency/efficiency roll-off/color rendering index/color-stability trade-off. *Phys. Status Solidi (RRL) Rapid Res. Lett.* **2014**, *8*, 719–723. [[CrossRef](#)]
45. Kim, H.S.; Cheon, H.J.; Lee, D.; Lee, W.; Kim, J.; Kim, Y.H.; Yoo, S. Toward highly efficient deep-blue OLEDs: Tailoring the multiresonance-induced TADF molecules for suppressed excimer formation and near-unity horizontal dipole ratio. *Sci. Adv.* **2023**, *9*, eadf1388. [[CrossRef](#)]
46. Xiao, P.; Huang, J.; Yu, Y.; Yuan, J.; Luo, D.; Liu, B.; Liang, D. Recent Advances of Exciplex-Based White Organic Light-Emitting Diodes. *Appl. Sci.* **2018**, *8*, 1449. [[CrossRef](#)]
47. Xu, T.; Fu, J.; Wang, X.; Lu, G.; Liu, B. Understanding the Structure and Energy Transfer Process of Undoped Ultrathin Emitting Nanolayers Within Interface Exciplexes. *Front. Chem.* **2022**, *10*, 887900. [[CrossRef](#)]
48. Matsumura, M.; Furukawa, T. Efficient Electroluminescence from a Rubrene Sub-Monolayer Inserted between Electron- and Hole-Transport Layers. *Jpn. Soc. Appl. Phys.* **2001**, *40*, 3211. [[CrossRef](#)]
49. Oyamada, T.; Maeda, C.; Sasabe, H.; Adachi, C. Efficient Electron Injection Mechanism in Organic Light-Emitting Diodes Using an Ultra Thin Layer of Low-Work-Function Metals. *Jpn. J. Appl. Phys.* **2003**, *42*, L1535. [[CrossRef](#)]
50. Xie, W.; Liu, S.; Zhao, Y. A nondoped-type small molecule white organic light-emitting device. *J. Phys. D Appl. Phys.* **2003**, *36*, 1246. [[CrossRef](#)]
51. Wu, Z.J.; Chen, S.F.; Yang, H.S.; Zhao, Y.; Li, C.N.; Hou, J.Y.; Liu, S.Y. Top-Emitting Organic Light-Emitting Devices Based on Silicon Substrate with High Luminance and Low Turn-on Voltage. *Chin. Phys. Lett.* **2005**, *22*, 233.
52. Xiao, B.; Li, C.; Li, X.; Ma, C.; Liu, S. Efficient Electroluminescence from a Quinacridone sub-monolayer inserted in a narrow exciton formation zone confined by a blocking layer. *Opt. Quant. Electron.* **2005**, *37*, 433–439. [[CrossRef](#)]
53. Yang, H. White organic light-emitting devices based on blue fluorescent dye combined with dual sub-monolayer. *J. Lumin.* **2013**, *142*, 231–235. [[CrossRef](#)]
54. Xue, Q.; Xie, G.; Liu, S.; Chen, P.; Zhao, Y.; Liu, S. Distinguishing triplet energy transfer and trap-assisted recombination in multi-color organic light-emitting diode with an ultrathin phosphorescent emissive layer. *J. Appl. Phys.* **2014**, *115*, 114504. [[CrossRef](#)]
55. Liu, B.; Sharma, M.; Yu, J.; Wang, L.; Shendre, S.; Sharma, A.; Izmir, M.; Delikanli, S.; Altintas, Y.; Dang, C.; et al. Management of electroluminescence from silver-doped colloidal quantum well light-emitting diodes. *Cell Rep. Phys. Sci.* **2022**, *3*, 100860. [[CrossRef](#)]
56. Liu, B.; Wang, L.; Xu, M.; Tao, H.; Zou, J.; Gao, D.; Lan, L.; Ning, H.; Peng, J.; Cao, Y. Efficient hybrid white organic light-emitting diodes with extremely long lifetime: The effect of n-type interlayer. *Sci. Rep.* **2014**, *4*, 7198. [[CrossRef](#)]
57. Sun, N.; Zhao, Y.; Zhao, F.; Chen, Y.; Yang, D.; Chen, J.; Ma, D. A white organic light-emitting diode with ultra-high color rendering index, high efficiency, and extremely low efficiency roll-off. *Appl. Phys. Lett.* **2014**, *105*, 013303. [[CrossRef](#)]
58. Du, X.; Tao, S.; Huang, Y.; Yang, X.; Ding, X.; Zhang, X. Efficient fluorescence/phosphorescence white organic light-emitting diodes with ultra high color stability and mild efficiency roll-off. *Appl. Phys. Lett.* **2015**, *107*, 183304. [[CrossRef](#)]
59. Xu, D.; Li, X.; Ju, H.; Zhu, Y.; Deng, Z. A novel red organic light-emitting diode with ultrathin DCJTb and Rubrene layers. *Displays* **2011**, *32*, 92–95. [[CrossRef](#)]
60. Xue, K.; Sheng, R.; Duan, Y.; Chen, P.; Chen, B.; Wang, X.; Duan, Y.; Zhao, Y. Efficient non-doped monochrome and white phosphorescent organic light-emitting diodes based on ultrathin emissive layers. *Org. Electron.* **2015**, *26*, 451–457. [[CrossRef](#)]
61. Liu, T.; Zhu, L.; Zhong, C.; Xie, G.; Gong, S.; Fang, J.; Ma, D.; Yang, C. Naphthothiadiazole-Based Near-Infrared Emitter with a Photoluminescence Quantum Yield of 60% in Neat Film and External Quantum Efficiencies of up to 3.9% in Nondoped OLEDs. *Adv. Funct. Mater.* **2017**, *27*, 1606384. [[CrossRef](#)]
62. Zhao, Y.; Wu, S.; Ling, Z.; Chen, H.; Yu, N.; Zhou, P.; Lian, H.; Lan, W.; Liao, Y.; Wei, B.; et al. Systematical Investigation of Ultrathin Doped Emissive Layer Structure: Achieving Highly Efficient and Long-Lifetime Orange Organic Light-Emitting Diodes. *Adv. Mater. Interfaces* **2019**, *7*, 1901609. [[CrossRef](#)]

63. Xue, K.; Han, G.; Duan, Y.; Chen, P.; Yang, Y.; Yang, D.; Duan, Y.; Wang, X.; Zhao, Y. Doping-free orange and white phosphorescent organic light-emitting diodes with ultra-simply structure and excellent color stability. *Org. Electron.* **2015**, *18*, 84–88. [[CrossRef](#)]
64. Wang, X.; Wang, R.; Zhou, D.; Yu, J. Study of organic light-emitting diodes with exciplex and non-exciplex forming interfaces consisting of an ultrathin rubrene layer. *Synth. Met.* **2016**, *214*, 50–55. [[CrossRef](#)]
65. Kidanu, H.T.; Chen, C.T. Achieving pure yellow, high-efficiency (EQE > 20%) electroluminescence from ultrathin emitting layer (0.6–2.0 nm) OLEDs having a rare aggregation-free heteroleptic platinum complex. *J. Mater. Chem. C* **2021**, *9*, 1410–1418. [[CrossRef](#)]
66. Zhang, T.; Shi, C.; Zhao, C.; Wu, Z.; Chen, J.; Xie, Z.; Ma, D. Extremely Low Roll-Off and High Efficiency Achieved by Strategic Exciton Management in Organic Light-Emitting Diodes with Simple Ultrathin Emitting Layer Structure. *ACS Appl. Mater. Interfaces* **2018**, *10*, 8148–8154. [[CrossRef](#)] [[PubMed](#)]
67. Liu, J.; Shi, X.; Wu, X.; Wang, J.; Min, Z.; Wang, Y.; Yang, M.; Chen, C.H.; He, G. Achieving above 30% external quantum efficiency for inverted phosphorescence organic light-emitting diodes based on ultrathin emitting layer. *Org. Electron.* **2014**, *15*, 2492–2498. [[CrossRef](#)]
68. Shi, X.; Liu, J.; Wang, J.; Wu, X.; Zheng, Y.; He, G. High efficiency green phosphorescent top-emitting organic light-emitting diode with ultrathin non-doped emissive layer. *Org. Electron.* **2014**, *15*, 2408–2413. [[CrossRef](#)]
69. Xu, T.; Zhou, J.G.; Huang, C.C.; Zhang, L.; Fung, M.K.; Murtaza, I.; Meng, H.; Liao, L.S. Highly Simplified Tandem Organic Light-Emitting Devices Incorporating a Green Phosphorescence Ultrathin Emitter within a Novel Interface Exciplex for High Efficiency. *ACS Appl. Mater. Interfaces* **2017**, *9*, 10955–10962. [[CrossRef](#)]
70. Nanda, G.P.; Sk, B.; Yadav, N.; Rajamanickam, S.; Deori, U.; Mahashaya, R.; Zysman Colman, E.; Rajamalli, P. Ultrathin non-doped thermally activated delayed fluorescence emitting layer for highly efficient OLEDs. *Chem. Commun.* **2021**, *57*, 13728–13731. [[CrossRef](#)]
71. Kang, S.W.; Baek, D.H.; Ju, B.K.; Park, Y.W. Green phosphorescent organic light-emitting diode exhibiting highest external quantum efficiency with ultra-thin undoped emission layer. *Sci. Rep.* **2021**, *11*, 8436. [[CrossRef](#)]
72. Wu, T.L.; Lei, J.; Hsieh, C.M.; Chen, Y.K.; Huang, P.Y.; Lai, P.T.; Chou, T.Y.; Lin, W.C.; Chen, W.; Yu, C.H.; et al. Substituent engineering of the diboron molecular architecture for a nondoped and ultrathin emitting layer. *Chem. Sci.* **2022**, *13*, 12996–13005. [[CrossRef](#)]
73. Ye, J.; Zheng, C.J.; Ou, X.M.; Zhang, X.H.; Fung, M.K.; Lee, C.S. Management of Singlet and Triplet Excitons in a Single Emission Layer: A Simple Approach for a High-Efficiency Fluorescence/Phosphorescence Hybrid White Organic Light-Emitting Device. *Adv. Mater.* **2012**, *24*, 3410–3414. [[CrossRef](#)] [[PubMed](#)]
74. Liu, B.Q.; Tao, H.; Su, Y.J.; Gao, D.Y.; Lan, L.F.; Zou, J.H.; Peng, J.B. Color-stable, reduced efficiency roll-off hybrid white organic light emitting diodes with ultra high brightness. *Chin. Phys. B* **2013**, *22*, 077303. [[CrossRef](#)]
75. Liu, B.; Nie, H.; Zhou, X.; Hu, S.; Luo, D.; Gao, D.; Zou, J.; Xu, M.; Wang, L.; Zhao, Z.; et al. Manipulation of Charge and Exciton Distribution Based on Blue Aggregation-Induced Emission Fluorophors: A Novel Concept to Achieve High-Performance Hybrid White Organic Light-Emitting Diodes. *Adv. Funct. Mater.* **2016**, *26*, 776–783. [[CrossRef](#)]
76. Chen, Y.; Chen, J.; Ma, D.; Yan, D.; Wang, L.; Zhu, F. High power efficiency tandem organic light-emitting diodes based on bulk heterojunction organic bipolar charge generation layer. *Appl. Phys. Lett.* **2011**, *98*, 243309. [[CrossRef](#)]
77. Zhang, X.; Zhang, M.; Liu, M.; Chen, Y.; Wang, J.; Zhang, X.; Zhang, J.; Lai, W.Y.; Huang, W. Highly efficient tandem organic light-emitting devices adopting a nondoped charge-generation unit and ultrathin emitting layers. *Org. Electron.* **2018**, *53*, 353–360. [[CrossRef](#)]
78. Zhang, S.; Yao, J.; Dai, Y.; Sun, Q.; Yang, D.; Qiao, X.; Chen, J.; Ma, D. High efficiency and color quality undoped phosphorescent white organic light-emitting diodes based on simple ultrathin structure in exciplex. *Org. Electron.* **2020**, *85*, 105821. [[CrossRef](#)]
79. Mu, H.; Jiang, Y.; Xie, H. Efficient blue phosphorescent organic light emitting diodes based on exciplex and ultrathin Firpic sandwiched layer. *Org. Electron.* **2019**, *66*, 195–205. [[CrossRef](#)]
80. Miao, Y.; Wang, G.; Yin, M.; Guo, Y.; Zhao, B.; Wang, H. Phosphorescent ultrathin emitting layers sensitized by TADF interfacial exciplex enables simple and efficient monochrome/white organic light-emitting diodes. *Chem. Eng. J.* **2023**, *461*, 141921. [[CrossRef](#)]
81. Liu, B.; Xu, Z.; Zou, J.; Tao, H.; Xu, M.; Gao, D.; Lan, L.; Wang, L.; Ning, H.; Peng, J. High-performance hybrid white organic light-emitting diodes employing p-type interlayers. *J. Ind. Eng. Chem.* **2015**, *27*, 240–244. [[CrossRef](#)]
82. Sasabe, H.; Kido, J. Development of high performance OLEDs for general lighting. *J. Mater. Chem. C* **2013**, *1*, 1699–1707. [[CrossRef](#)]
83. Liu, B.; Wang, L.; Gao, D.; Xu, M.; Zhu, X.; Zou, J.; Lan, L.; Ning, H.; Peng, J.; Cao, Y. Harnessing charge and exciton distribution towards extremely high performance: The critical role of guests in single-emitting-layer white OLEDs. *Mater. Horiz.* **2015**, *2*, 536–544. [[CrossRef](#)]
84. Liu, B.; Luo, D.; Zou, J.; Gao, D.; Ning, H.; Wang, L.; Peng, J.; Cao, Y. A host–guest system comprising high guest concentration to achieve simplified and high-performance hybrid white organic light-emitting diodes. *J. Mater. Chem. C* **2015**, *3*, 6359–6366. [[CrossRef](#)]
85. Schwartz, G.; Pfeiffer, M.; Reineke, S.; Walzer, K.; Leo, K. Harvesting Triplet Excitons from Fluorescent Blue Emitters in White Organic Light-Emitting Diodes. *Adv. Mater.* **2007**, *19*, 3672–3676. [[CrossRef](#)]
86. Liu, B.; Xu, M.; Wang, L.; Tao, H.; Su, Y.; Gao, D.; Lan, L.; Zou, J.; Peng, J. Very-High Color Rendering Index Hybrid White Organic Light-Emitting Diodes with Double Emitting Nanolayers. *Nano-Micro Lett.* **2014**, *6*, 335–339. [[CrossRef](#)]

87. Liu, B.; Wang, L.; Gao, D.; Zou, J.; Ning, H.; Peng, J.; Cao, Y. Extremely high-efficiency and ultrasimplified hybrid white organic light-emitting diodes exploiting double multifunctional blue emitting layers. *Light Sci. Appl.* **2016**, *5*, e16137. [[CrossRef](#)]
88. Zhao, Y.; Chen, J.; Ma, D. Ultrathin Nondoped Emissive Layers for Efficient and Simple Monochrome and White Organic Light-Emitting Diodes. *ACS Appl. Mater. Interfaces* **2013**, *5*, 965–971. [[CrossRef](#)]
89. Zhu, L.; Zhao, Y.; Zhang, H.; Chen, J.; Ma, D. Using an ultra-thin non-doped orange emission layer to realize high efficiency white organic light-emitting diodes with low efficiency roll-off. *J. Appl. Phys.* **2014**, *115*, 244512. [[CrossRef](#)]
90. Liu, B.; Xu, M.; Wang, L.; Su, Y.; Gao, D.; Tao, H.; Lan, L.; Zou, J.; Peng, J. High-Performance Hybrid White Organic Light-Emitting Diodes Comprising Ultrathin Blue and Orange Emissive Layers. *Appl. Phys. Express* **2013**, *6*, 122101. [[CrossRef](#)]
91. Wang, J.; Li, W. Adjusting White OLEDs with Yellow Light Emission Phosphor Dye and Ultrathin NPB Layer Structure. *Int. J. Photoenergy* **2013**, *2013*, 639843. [[CrossRef](#)]
92. Liu, S.; Yu, J.; Ma, Z.; Zhao, J. Highly efficient white organic light-emitting devices consisting of undoped ultrathin yellow phosphorescent layer. *J. Lumin.* **2013**, *134*, 665–669. [[CrossRef](#)]
93. Jeon, T.; Geffroy, B.; Tondelier, D.; Bonnassieux, Y.; Forget, S.; Chenais, S.; Ishow, E. White organic light-emitting diodes with an ultra-thin premixed emitting layer. *Thin Solid Films* **2013**, *542*, 263–269. [[CrossRef](#)]
94. Zhao, F.; Zhu, L.; Liu, Y.; Wang, Y.; Ma, D. Doping-free hybrid white organic light-emitting diodes with fluorescent blue, phosphorescent green and red emission layers. *Org. Electron.* **2015**, *27*, 207–211. [[CrossRef](#)]
95. Xu, L.; Tang, C.W.; Rothberg, L.J. High efficiency phosphorescent white organic light-emitting diodes with an ultra-thin red and green co-doped layer and dual blue emitting layers. *Org. Electron.* **2016**, *32*, 54–58. [[CrossRef](#)]
96. Xu, T.; Yang, M.; Liu, J.; Wu, X.; Murtaza, I.; He, G.; Meng, H. Wide color-range tunable and low roll-off fluorescent organic light emitting devices based on double undoped ultrathin emitters. *Org. Electron.* **2016**, *37*, 93–99. [[CrossRef](#)]
97. Sheng, R.; Zuo, L.; Xue, K.; Duan, Y.; Chen, P.; Cheng, G.; Zhao, Y. Efficient white phosphorescent organic light-emitting diodes consisting of orange ultrathin and blue mixed host emission layers. *J. Phys. D Appl. Phys.* **2016**, *49*, 335101. [[CrossRef](#)]
98. Tao, P.; Miao, Y.; Zhang, Y.; Wang, K.; Li, H.; Li, L.; Li, X.; Yang, T.; Zhao, Q.; Wang, H.; et al. Highly efficient thienylquinoline-based phosphorescent iridium(III) complexes for red and white organic light-emitting diodes. *Org. Electron.* **2017**, *45*, 293–301. [[CrossRef](#)]
99. Zhang, H.; Yang, X.; Cheng, J.; Li, D.; Chen, H.; Yu, J.; Li, L. Enhanced color stability for white organic light-emitting diodes based on dual ultra-thin emitting layer. *Org. Electron.* **2017**, *50*, 147–152. [[CrossRef](#)]
100. Xue, K.; Sheng, R.; Chen, B.; Duan, Y.; Chen, P.; Yang, Y.; Wang, X.; Duan, Y.; Zhao, Y. Improved performance for white phosphorescent organic light-emitting diodes utilizing an orange ultrathin non-doped emission layer. *RSC Adv.* **2015**, *5*, 39097. [[CrossRef](#)]
101. Tan, T.; Ouyang, S.; Xie, Y.; Wang, D.; Zhu, D.; Xu, X.; Fong, H.H. Balanced white organic light-emitting diode with non-doped ultra-thin emissive layers based on exciton management. *Org. Electron.* **2015**, *25*, 232–236. [[CrossRef](#)]
102. Liu, B.; Tao, H.; Wang, L.; Gao, D.; Liu, W.; Zou, J.; Xu, M.; Ning, H.; Peng, J.; Cao, Y. High-performance doping-free hybrid white organic light-emitting diodes: The exploitation of ultrathin emitting nanolayers (<1 nm). *Nano Energy* **2016**, *26*, 26–36. [[CrossRef](#)]
103. Yang, X.; Zhang, X.; Deng, J.; Chu, Z.; Jiang, Q.; Meng, J.; Wang, P.; Zhang, L.; Yin, Z.; You, J. Efficient green light-emitting diodes based on quasi-two-dimensional composition and phase engineered perovskite with surface passivation. *Nat. Commun.* **2018**, *9*, 570. [[CrossRef](#)]
104. Xiao, P.; Huang, J.; Yu, Y.; Liu, B. Recent Developments in Tandem White Organic Light-Emitting Diodes. *Molecules* **2019**, *24*, 151. [[CrossRef](#)] [[PubMed](#)]
105. Ji, W.; Liu, S.; Zhang, H.; Wang, R.; Xie, W.; Zhang, H. Ultrasonic Spray Processed, Highly Efficient All-Inorganic Quantum Dot Light-Emitting Diodes. *ACS Photonics* **2017**, *4*, 1271–1278. [[CrossRef](#)]
106. Liu, B.; Wang, L.; Xu, M.; Tao, H.; Xia, X.; Zou, J.; Su, Y.; Gao, D.; Lan, L.; Peng, J. Simultaneous achievement of low efficiency roll-off and stable color in highly efficient single-emitting-layer phosphorescent white organic light-emitting diodes. *J. Mater. Chem. C* **2014**, *2*, 5870–5877. [[CrossRef](#)]
107. Tang, X.; Pan, R.; Zhu, H.; Zhao, X.; Tu, L.; Xiong, Z. The origin of interlayer-induced significant enhancement of EQE in CzDBA-based OLEDs studied by magneto-electroluminescence. *Appl. Phys. Lett.* **2021**, *118*, 013503. [[CrossRef](#)]
108. Miao, Y.; Wang, K.; Gao, L.; Wang, H.; Zhu, F.; Xu, B. Non-phosphor-doped fluorescent/phosphorescent hybrid white organic lightemitting diodes with a sandwiched blue emitting layer for simultaneously achieving superior device efficiency and color quality. *J. Mater. Chem. C* **2018**, *6*, 9811–9820. [[CrossRef](#)]
109. Yu, H.; Dai, X.; Yao, F.; Wei, X.; Cao, J.; Jhun, C. Efficient white phosphorescent organic light-emitting diodes using ultrathin emissive layers (<1 nm). *Sci. Rep.* **2018**, *8*, 6068.
110. Dai, X.; Yao, F.; Li, J.; Yu, H.; Cao, J. Color-stable non-doped white phosphorescent organic light-emitting diodes based on ultrathin emissive layers. *J. Phys. D Appl. Phys.* **2020**, *53*, 055106. [[CrossRef](#)]
111. Dai, X.; Cao, J. Study on spectral stability of white organic light-emitting diodes with mixed bipolar spacer based on ultrathin non-doped phosphorescent emitting layers. *Org. Electron.* **2020**, *78*, 105563. [[CrossRef](#)]
112. Wu, S.; Li, S.; Sun, Q.; Huang, C.; Fung, M.K. Highly Efficient White Organic Light-Emitting Diodes with Ultrathin Emissive Layers and a Spacer-Free Structure. *Sci. Rep.* **2016**, *6*, 25821. [[CrossRef](#)]
113. Chen, Y.; Ma, D.; Sun, H.; Chen, J.; Guo, Q.; Wang, Q.; Zhao, Y. Organic semiconductor heterojunctions: Electrode-independent charge injectors for high-performance organic light-emitting diodes. *Light Sci. Appl.* **2016**, *5*, e16042. [[CrossRef](#)]

114. Liu, B.; Xu, M.; Tao, H.; Ying, L.; Zou, J.; Wu, H.; Peng, J. Highly efficient red phosphorescent organic light-emitting diodes based on solution processed emissive layer. *J. Lumin.* **2013**, *142*, 35–39. [[CrossRef](#)]
115. Liu, B.; Xu, M.; Wang, L.; Tao, H.; Su, Y.; Gao, D.; Zou, J.; Lan, L.; Peng, J. Comprehensive Study on the Electron Transport Layer in Blue Fluorescent Organic Light-Emitting Diodes. *ECS J. Solid State Sci. Technol.* **2013**, *2*, R258. [[CrossRef](#)]
116. Liu, B.; Zou, J.; Zhou, Z.; Wang, L.; Xu, M.; Tao, H.; Gao, D.; Lan, L.; Ning, H.; Peng, J. Efficient single-emitting layer hybrid white organic light-emitting diodes with low efficiency roll-off, stable color and extremely high luminance. *J. Ind. Eng. Chem.* **2015**, *30*, 85–91. [[CrossRef](#)]
117. Wen, Z.; Zhang, C.; Zhou, Z.; Xu, B.; Wang, K.; Teo, K.L.; Sun, X.W. Ultrapure Green Light-Emitting Diodes Based on CdSe/CdS Core/Crown Nanoplatelets. *IEEE J. Quant. Electron.* **2020**, *56*, 1–6. [[CrossRef](#)]
118. Wang, B.; Kou, Z.; Tang, Y.; Yang, F.; Fu, X.; Yuan, Q. High CRI and stable spectra white organic light-emitting diodes with double doped blue emission layers and multiple ultrathin phosphorescent emission layers by adjusting the thickness of spacer layer. *Org. Electron.* **2019**, *70*, 149–154. [[CrossRef](#)]
119. Miao, Y.; Tao, P.; Wang, K.; Li, H.; Zhao, B.; Gao, L.; Wang, H.; Xu, B.; Zhao, Q. Highly Efficient Red and White Organic Light-Emitting Diodes with External Quantum Efficiency beyond 20% by Employing Pyridylimidazole-Based Metallophosphors. *ACS Appl. Mater. Interfaces* **2017**, *9*, 37873–37882. [[CrossRef](#)] [[PubMed](#)]
120. Miao, Y.; Wang, K.; Zhao, B.; Gao, L.; Tao, P.; Liu, X.; Hao, Y.; Wang, H.; Xu, B.; Zhu, F. High-efficiency/CRI/color stability warm white organic light-emitting diodes by incorporating ultrathin phosphorescence layers in a blue fluorescence layer. *Nanophotonics* **2017**, *7*, 295–304. [[CrossRef](#)]
121. Zhang, T.; Shi, C.; Zhao, C.; Wu, Z.; Sun, N.; Chen, J.; Xie, Z.; Ma, D. High efficiency phosphorescent white organic light-emitting diodes with low efficiency roll-off achieved by strategic exciton management based on simple ultrathin emitting layer structures. *J. Mater. Chem. C* **2017**, *5*, 12833–12838. [[CrossRef](#)]
122. Zhao, B.; Zhang, H.; Wang, Z.; Miao, Y.; Wang, Z.; Li, J.; Wang, H.; Hao, Y.; Li, W. Non-doped white organic light-emitting diodes with superior efficiency/color stability by employing ultra-thin phosphorescent emitters. *J. Mater. Chem. C* **2018**, *6*, 4250–4256. [[CrossRef](#)]
123. Luo, D.; Chen, Q.; Liu, B.; Qiu, Y. Emergence of Flexible White Organic Light-Emitting Diodes. *Polymers* **2019**, *11*, 384. [[CrossRef](#)]
124. Liu, B.; Wang, L.; Tao, H.; Xu, M.; Zou, J.; Ning, H.; Peng, J.; Cao, Y. Doping-free tandem white organic light-emitting diodes. *Chin. Sci. Bull.* **2017**, *62*, 1193–1200. [[CrossRef](#)]
125. Kidanu, H.T.; Chen, C.T. Solid-state near infrared emitting platinum(II) complexes as either an ultrathin or singly doped phosphorescence emitting layer in hybrid white OLEDs exhibiting high efficiency and colour rendering index. *J. Mater. Chem. C* **2021**, *9*, 15470–15476. [[CrossRef](#)]
126. Liu, B.; Nie, H.; Lin, G.; Hu, S.; Gao, D.; Zou, J.; Xu, M.; Wang, L.; Zhao, Z.; Ning, H.; et al. High-Performance Doping-Free Hybrid White OLEDs Based on Blue Aggregation-Induced Emission Luminogens. *ACS Appl. Mater. Interfaces* **2017**, *9*, 34162–34171. [[CrossRef](#)]
127. Ying, S.; Yao, J.; Chen, Y.; Ma, D. High efficiency ($\sim 100 \text{ lm W}^{-1}$) hybrid WOLEDs by simply introducing ultrathin non-doped phosphorescent emitters in a blue exciplex host. *J. Mater. Chem. C* **2018**, *6*, 7070–7076. [[CrossRef](#)]
128. Chen, Y.; Wu, Y.; Lin, C.; Dai, Y.; Sun, Q.; Yang, D.; Qiao, X.; Ma, D. Simultaneous high efficiency/CRI/spectral stability and low efficiency roll-off hybrid white organic light-emitting diodes via simple insertion of ultrathin red/green phosphorescent emitters in a blue exciplex. *J. Mater. Chem. C* **2020**, *8*, 12450–12456. [[CrossRef](#)]
129. Zhao, C.; Yan, D.; Ahamad, T.; Alshehri, S.M.; Ma, D. High efficiency and low roll-off hybrid white organic light emitting diodes by strategically introducing multi-ultrathin phosphorescent layers in blue exciplex emitter. *J. Appl. Phys.* **2019**, *125*, 045501. [[CrossRef](#)]
130. Liu, Z.; Zhao, B.; Gao, Y.; Chen, H.; Dong, B.; Xu, Y.; Wang, H.; Xu, B.; Li, W. Modulation for efficiency and spectra of non-doped white organic light emitting diodes by combining an exciplex with an ultrathin phosphorescent emitter. *RSC Adv.* **2020**, *10*, 33461–33468. [[CrossRef](#)]
131. Ying, S.; Chen, Y.; Yao, J.; Sun, Q.; Dai, Y.; Yang, D.; Qiao, X.; Chen, J.; Ma, D. High efficiency doping-free warm-white organic light-emitting diodes with strategic-tuning of radiative excitons by combining interfacial exciplex with multi-ultrathin emissive layers. *Org. Electron.* **2020**, *85*, 105876. [[CrossRef](#)]
132. Zhang, L.; Xiao, W.; Wu, W.; Liu, B. Research Progress on Flexible Oxide-Based Thin Film Transistors. *Appl. Sci.* **2019**, *9*, 773. [[CrossRef](#)]
133. Guo, J.; Li, X.; Nie, H.; Luo, W.; Gan, S.; Hu, S.; Hu, R.; Qin, A.; Zhao, Z.; Su, S.; et al. Achieving High-Performance Nondoped OLEDs with Extremely Small Efficiency Roll-Off by Combining Aggregation-Induced Emission and Thermally Activated Delayed Fluorescence. *Adv. Funct. Mater.* **2017**, *27*, 1606458. [[CrossRef](#)]
134. Liao, X.; An, K.; Cheng, J.; Li, Y.; Meng, X.; Yang, X.; Li, L. High efficiency ultra-thin doping-free WOLED based on blue thermally activated delayed fluorescence inter-layer switch. *Appl. Surf. Sci.* **2019**, *487*, 610–615. [[CrossRef](#)]
135. Zhao, J.; Wang, Z.; Wang, R.; Chi, Z.; Yu, J. Hybrid white organic light-emitting devices consisting of a non-doped thermally activated delayed fluorescent emitter and an ultrathin phosphorescent emitter. *J. Lumin.* **2017**, *184*, 287–292. [[CrossRef](#)]
136. Xue, C.; Zhang, G.; Jiang, W.; Lang, J.; Jiang, X. High performance non-doped blue-hazard-free hybrid white organic light-emitting diodes with stable high color rendering index and low efficiency roll-off. *Opt. Mater.* **2020**, *106*, 109991. [[CrossRef](#)]

137. Zhang, J.; Wang, Y.; Liu, S.; Yu, H.; Zhang, L.; Xie, W. Color-tunable organic light-emitting diodes with ultrathin thermal activation delayed fluorescence emitting layer. *Appl. Phys. Lett.* **2022**, *120*, 171102. [[CrossRef](#)]
138. Sheng, R.; Yang, L.; Li, A.; Chen, K.; Zhang, F.; Duan, Y.; Zhao, Y.; Chen, P. Highly efficient orange and white OLEDs based on ultrathin phosphorescent emitters with double reverse intersystem crossing system. *J. Lumin.* **2022**, *246*, 118852. [[CrossRef](#)]
139. Sun, W.; Chen, K.; Li, S.; Sun, Y.; Liu, W.; Jiao, S.; Zhou, L. Efficient hybrid white organic light-emitting diodes with superior color stability and slow efficiency roll-off based on ultrathin emitting layer structures. *J. Lumin.* **2022**, *249*, 119053. [[CrossRef](#)]
140. Perumal, A.; Shendre, S.; Li, M.J.; Tay, Y.K.E.; Sharma, V.K.; Chen, S.; Wei, Z.; Liu, Q.; Gao, Y.; Buenconsejo, P.J.S.; et al. High brightness formamidinium lead bromide perovskite nanocrystal light emitting devices. *Sci. Rep.* **2016**, *6*, 36733. [[CrossRef](#)]
141. Fang, Z.B.; Chen, W.J.; Shi, Y.L.; Zhao, J.; Chu, S.L.; Zhang, J.; Xiao, Z.G. Dual Passivation of Perovskite Defects for Light-Emitting Diodes with External Quantum Efficiency Exceeding 20%. *Adv. Funct. Mater.* **2020**, *30*, 1909754. [[CrossRef](#)]
142. Zhang, C.; Kuang, D.B.; Wu, W.Q. A Review of Diverse Halide Perovskite Morphologies for Efficient Optoelectronic Applications. *Small Methods* **2020**, *4*, 1900662. [[CrossRef](#)]
143. Hu, Y.; Wang, Q.; Shi, Y.L.; Li, M.; Zhang, L.; Wang, Z.K.; Liao, L.S. Vacuum-evaporated all-inorganic cesium lead bromine perovskites for high-performance light-emitting diodes. *J. Mater. Chem. C* **2017**, *5*, 8144–8149. [[CrossRef](#)]
144. Cao, Y.; Wang, N.; Tian, H.; Guo, J.; Wei, Y.; Chen, H.; Miao, Y.; Zou, W.; Pan, K.; He, Y.; et al. Perovskite light-emitting diodes based on spontaneously formed submicrometre-scale structures. *Nature* **2018**, *562*, 249–253. [[CrossRef](#)] [[PubMed](#)]
145. Yang, X.L.; Zhou, G.J.; Wong, W.Y. Functionalization of phosphorescent emitters and their host materials by main-group elements for phosphorescent organic light-emitting devices. *Chem. Soc. Rev.* **2015**, *44*, 8484–8575. [[CrossRef](#)]
146. Jou, J.H.; Kumar, S.; Agrawal, A.; Li, T.H.; Sahoo, S. Approaches for fabricating high efficiency organic light emitting diodes. *J. Mater. Chem. C* **2015**, *3*, 2974–3002. [[CrossRef](#)]
147. Wei, Z.; Xing, J. The Rise of Perovskite Light-Emitting Diodes. *J. Phys. Chem. Lett.* **2019**, *10*, 3035–3042. [[CrossRef](#)]
148. Jeon, S.K.; Lee, H.M.; Yook, K.S.; Lee, J.Y. Recent Progress of the Lifetime of Organic Light-Emitting Diodes Based on Thermally Activated Delayed Fluorescent Material. *Adv. Mater.* **2019**, *31*, 1803524. [[CrossRef](#)]
149. Shen, H.; Gao, Q.; Zhang, Y.; Lin, Y.; Lin, Q.; Li, Z.; Chen, L.; Zeng, Z.; Li, X.; Jia, Y.; et al. Visible quantum dot light-emitting diodes with simultaneous high brightness and efficiency. *Nat. Photonics* **2019**, *13*, 192–197. [[CrossRef](#)]
150. Wang, K.H.; Zhu, B.S.; Yao, J.S.; Yao, H.B. Chemical regulation of metal halide perovskite nanomaterials for efficient light-emitting diodes. *Sci. China Chem.* **2018**, *61*, 1047–1061. [[CrossRef](#)]
151. van Le, Q.; Jang, H.W.; Kim, S.Y. Recent Advances toward High-Efficiency Halide Perovskite Light-Emitting Diodes: Review and Perspective. *Small Methods* **2018**, *2*, 1700419. [[CrossRef](#)]
152. Zhao, X.F.; Ng, J.D.A.; Friend, R.H.; Tan, Z.K. Opportunities and Challenges in Perovskite Light-Emitting Devices. *ACS Photonics* **2018**, *5*, 3866–3875. [[CrossRef](#)]
153. Wang, H.; Zhang, X.; Wu, Q.; Cao, F.; Yang, D.; Shang, Y.; Ning, Z.; Zhang, W.; Zheng, W.; Yan, Y.; et al. Trifluoroacetate induced small-grained CsPbBr₃ perovskite films result in efficient and stable light-emitting devices. *Nat. Commun.* **2019**, *10*, 665. [[CrossRef](#)] [[PubMed](#)]
154. Wei, Y.; Cheng, Z.Y.; Lin, J. An overview on enhancing the stability of lead halide perovskite quantum dots and their applications in phosphor-converted LEDs. *Chem. Soc. Rev.* **2019**, *48*, 310–350. [[CrossRef](#)] [[PubMed](#)]
155. Wang, Q.; Ma, D. Management of charges and excitons for high-performance white organic light-emitting diodes. *Chem. Soc. Rev.* **2010**, *39*, 2387–2398. [[CrossRef](#)]
156. Li, X.L.; Xie, G.; Liu, M.; Chen, D.; Cai, X.; Peng, J.; Cao, Y.; Su, S.J. High-Efficiency WOLEDs with High Color-Rendering Index based on a Chromaticity-Adjustable Yellow Thermally Activated Delayed Fluorescence Emitter. *Adv. Mater.* **2016**, *28*, 4614–4619. [[CrossRef](#)]
157. Shirasaki, Y.; Supran, G.J.; Bawendi, M.G.; Bulović, V. Emergence of colloidal quantum-dot light-emitting technologies. *Nat. Photonics* **2013**, *7*, 13–23. [[CrossRef](#)]
158. Yang, Y.; Zheng, Y.; Cao, W.R.; Titov, A.; Hyvonen, J.; Manders, J.R.; Xue, X.; Holloway, P.H.; Qian, L. High-efficiency light-emitting devices based on quantum dots with tailored nanostructures. *Nat. Photonics* **2015**, *9*, 259–266. [[CrossRef](#)]
159. Hames, B.C.; Sanchez, R.S.; Fakharuddin, A.; Mora Sero, I. A Comparative Study of Light-Emitting Diodes Based on All-Inorganic Perovskite Nanoparticles (CsPbBr₃) Synthesized at Room Temperature and by a Hot-Injection Method. *Chempluschem* **2018**, *83*, 294–299. [[CrossRef](#)]
160. Shen, X.; Zhang, Y.; Kershaw, S.V.; Li, T.; Wang, C.; Zhang, X.; Wang, W.; Li, D.; Wang, Y.; Lu, M.; et al. Zn-Alloyed CsPbI₃ Nanocrystals for Highly Efficient Perovskite Light-Emitting Devices. *Nano Lett.* **2019**, *19*, 1552–1559. [[CrossRef](#)]
161. Zhang, X.; Wang, W.; Xu, B.; Liu, S.; Dai, H.; Bian, D.; Chen, S.; Wang, K.; Sun, X. Thin film perovskite light-emitting diode based on CsPbBr₃ powders and interfacial engineering. *Nano Energy* **2017**, *37*, 40–45. [[CrossRef](#)]
162. Koo, J.R.; Lee, S.J.; Lee, H.W.; Lee, D.H.; Yang, H.J.; Kim, W.Y.; Kim, Y.K. Flexible bottom-emitting white organic light-emitting diodes with semitransparent Ni/Ag/Ni anode. *Opt. Express* **2013**, *21*, 11086–11094. [[CrossRef](#)]
163. Ou, Q.D.; Zhou, L.; Li, Y.Q.; Chen, S.; Chen, J.D.; Li, C.; Wang, Q.K.; Lee, S.T.; Tang, J.X. Extremely Efficient White Organic Light-Emitting Diodes for General Lighting. *Adv. Funct. Mater.* **2014**, *24*, 7249–7256. [[CrossRef](#)]
164. Wierer, J.J., Jr.; David, A.; Megens, M.M. III-nitride photonic-crystal light-emitting diodes with high extraction efficiency. *Nat. Photonics* **2009**, *3*, 163–169. [[CrossRef](#)]

165. Seo, S.W.; Jung, E.; Seo, S.J.; Chae, H.; Chung, H.K.; Cho, S.M. Toward fully flexible multilayer moisture-barriers for organic light-emitting diodes. *Jpn. J. Appl. Phys.* **2013**, *114*, 143505. [[CrossRef](#)]
166. Lu, M.; Zhang, Y.; Wang, S.X.; Guo, J.; Yu, W.W.; Rogach, A.L. Metal Halide Perovskite Light-Emitting Devices: Promising Technology for Next-Generation Displays. *Adv. Funct. Mater.* **2019**, *29*, 1902008. [[CrossRef](#)]
167. Yang, D.; Cao, M.; Zhong, Q.X.; Li, P.L.; Zhang, X.H.; Zhang, Q. All-inorganic cesium lead halide perovskite nanocrystals: Synthesis, surface engineering and applications. *J. Mater. Chem. C* **2019**, *7*, 757–789. [[CrossRef](#)]
168. Yao, J.; Dong, S.C.; Tam, B.S.T.; Tang, C.W. Lifetime Enhancement and Degradation Study of Blue OLEDs Using Deuterated Materials. *ACS Appl. Mater. Interfaces* **2023**, *15*, 7255–7262. [[CrossRef](#)]
169. Jeon, Y.; Choi, H.R.; Park, K.C.; Choi, K.C. Flexible organic light-emitting-diode-based photonic skin for attachable phototherapeutics. *J. Soc. Inf. Disp.* **2020**, *28*, 324–332. [[CrossRef](#)]
170. Swayamprabha, S.S.; Dubey, D.K.; Shah Nawaz, R.A.K.; Yadav, R.A.K.; Nagar, M.R.; Sharma, A.; Tung, F.; Jou, J.H. Approaches for Long Lifetime Organic Light Emitting Diodes. *Adv. Sci.* **2020**, *8*, 2002254. [[CrossRef](#)]
171. Jou, J.; Lin, Y.; Su, Y.; Song, W.; Kumar, S.; Dubey, D.K.; Shyue, J.; Chang, H.; You, Y.; Liang, T. Plausible degradation mechanisms in organic light-emitting diodes. *Org. Electron.* **2019**, *67*, 222–231. [[CrossRef](#)]
172. Jou, J.; Tai, T.; Su, Y.; Yu, H.; Chiang, C.; Chavhan, S.D.; Lin, Y.; Shyue, J.; Liang, T. Back Migration Based Long Lifetime Approach for Organic Light-Emitting Diode. *Phys. Status Solidi A* **2019**, *216*, 1800390. [[CrossRef](#)]
173. Vijaya Sundar, J.; Subramanian, V.; Rajakumar, B. Excited state C-N bond dissociation and cyclization of tri-aryl amine-based OLED materials: A theoretical investigation. *Phys. Chem. Chem. Phys.* **2018**, *21*, 438–447. [[CrossRef](#)] [[PubMed](#)]
174. Azrain, M.M.; Mansor, M.R.; Omar, G.; Fadzullah, S.H.S.M.; Esa, S.R.; Lim, L.M.; Sivakumar, D.; Nordin, M.N.A. Effect of high thermal stress on the organic light emitting diodes (OLEDs) performances. *Synth. Met.* **2019**, *247*, 191–201. [[CrossRef](#)]
175. Mizukami, M.; Cho, S.I.; Watanabe, K.; Abiko, M.; Suzuri, Y.; Tokito, S.; Kido, J. Flexible Organic Light-Emitting Diode Displays Driven by Inkjet-Printed High-Mobility Organic Thin-Film Transistors. *IEEE Electron. Device Lett.* **2017**, *39*, 39–42. [[CrossRef](#)]
176. Kim, E.; Han, Y.; Kim, W.; Choi, K.C.; Im, H.G.; Bae, B.S. Thin film encapsulation for organic light emitting diodes using a multi-barrier composed of MgO prepared by atomic layer deposition and hybrid materials. *Org. Electron.* **2013**, *14*, 1737–1743. [[CrossRef](#)]
177. Sun, Q.J.; Wang, Y.A.; Li, L.S.; Wang, D.Y.; Zhu, T.; Xu, J.; Yang, C.H.; Li, Y.F. Bright, multicoloured light-emitting diodes based on quantum dots. *Nat. Photonics* **2007**, *1*, 717–722. [[CrossRef](#)]
178. Kim, J.H.; Han, S.H.; Lee, J.Y. Concentration quenching resistant donor-acceptor molecular structure for high efficiency and long lifetime thermally activated delayed fluorescent organic light-emitting diodes via suppressed non-radiative channel. *Chem. Eng. J.* **2020**, *395*, 125159. [[CrossRef](#)]
179. Chu, T.Y.; Chen, J.F.; Chen, S.Y.; Chen, C.H. Comparative study of single and multiemissive layers in inverted white organic light-emitting devices. *Appl. Phys. Lett.* **2006**, *89*, 113502. [[CrossRef](#)]
180. Yu, J.N.; Zhang, M.Y.; Li, C.; Shang, Y.Z.; Lu, Y.F.; Wei, B.; Huang, W. Fine-tuning the thicknesses of organic layers to realize high-efficiency and long-lifetime blue organic light-emitting diodes. *Chin. Phys. B* **2012**, *21*, 083303. [[CrossRef](#)]
181. Mai, R.; Wu, X.; Jiang, Y.; Meng, Y.; Liu, B.; Hu, X.; Roncali, J.; Zhou, G.; Liu, J.M.; Kempa, K.; et al. An efficient multi-functional material based on polyether-substituted indolocarbazole for perovskite solar cells and solution-processed non-doped OLEDs. *J. Mater. Chem. A* **2019**, *7*, 1539–1547. [[CrossRef](#)]
182. Liu, B.; Xu, M.; Tao, H.; Su, Y.; Gao, D.; Zou, J.; Lan, L.; Peng, J. The effect of spacer in hybrid white organic light emitting diodes. *Chin. Sci. Bull.* **2014**, *59*, 3090–3097. [[CrossRef](#)]
183. Zhou, J.; Zou, J.; Dai, C.; Zhang, Y.; Luo, X.; Liu, B. High-Efficiency and High-Luminance Three-Color White Organic Light-Emitting Diodes with Low Efficiency Roll-Off. *ECS J. Solid State Sci. Technol.* **2018**, *7*, R99. [[CrossRef](#)]
184. Liu, B.; Sharma, M.; Yu, J.; Shendre, S.; Hettiarachchi, C.; Sharma, A.; Yeltik, A.; Wang, L.; Sun, H.; Dang, C.; et al. Light-Emitting Diodes with Cu-Doped Colloidal Quantum Wells: From Ultrapure Green, Tunable Dual-Emission to White Light. *Small* **2019**, *15*, e1901983. [[CrossRef](#)] [[PubMed](#)]
185. Liu, B.; Altintas, Y.; Wang, L.; Shendre, S.; Sharma, M.; Sun, H.; Mutlugun, E.; Demir, H.V. Record High External Quantum Efficiency of 19.2% Achieved in Light-Emitting Diodes of Colloidal Quantum Wells Enabled by Hot-Injection Shell Growth. *Adv. Mater.* **2020**, *32*, e1905824. [[CrossRef](#)]
186. Ohno, Y. Color rendering and luminous efficacy of white LED spectra. In Proceedings of the Fourth International Conference on Solid State Lighting, Denver, CO, USA, 2–6 August 2004.
187. Chen, B.; Liu, B.; Zeng, J.; Nie, H.; Xiong, Y.; Zou, J.; Ning, H.; Wang, Z.; Zhao, Z.; Tang, B.Z. Efficient Bipolar Blue AIEgens for High-Performance Nondoped Blue OLEDs and Hybrid White OLEDs. *Adv. Funct. Mater.* **2018**, *28*, 1803369. [[CrossRef](#)]
188. Shi, Z.; Li, Y.; Zhang, Y.; Chen, Y.; Li, X.; Wu, D.; Xu, T.; Shan, C.; Du, G. High-Efficiency and Air-Stable Perovskite Quantum Dots Light-Emitting Diodes with an All-Inorganic Heterostructure. *Nano Lett.* **2017**, *17*, 313–321. [[CrossRef](#)]
189. Ding, L.; Wang, J.N.; Ni, T.; Xue, Q.; Hu, S.; Wu, R.; Luo, D.; Zheng, H.; Liu, Y.; Liu, B. Extremely-low-voltage, high-efficiency and stability-enhanced inverted bottom OLEDs enabled via a p-type/ultra-thin metal/n-doped electron injection layer. *J. Mater. Chem. C* **2023**, *11*, 2672–2679. [[CrossRef](#)]
190. Park, J.S.; Chae, H.; Chung, H.K.; Lee, S.I. Thin film encapsulation for flexible AM-OLED: A review. *Semicond. Sci. Technol.* **2011**, *26*, 034001. [[CrossRef](#)]

191. Liu, B.; Wang, L.; Xu, M.; Tao, H.; Gao, D.; Zou, J.; Lan, L.; Ning, H.; Peng, J.; Cao, Y. Extremely stable-color flexible white organic light-emitting diodes with efficiency exceeding 100 lm W^{-1} . *J. Mater. Chem. C* **2014**, *2*, 9836. [[CrossRef](#)]
192. Hu, S.; Shabani, F.; Liu, B.; Zhang, L.; Guo, M.; Lu, G.; Zhou, Z.; Wang, J.; Huang, J.C.; Min, Y.; et al. High-performance deep red colloidal quantum well light-emitting diodes enabled by the understanding of charge dynamics. *ACS Nano* **2022**, *16*, 10840. [[CrossRef](#)] [[PubMed](#)]
193. Tao, H.; Gao, D.Y.; Liu, B.Q.; Wang, L.; Zou, J.H.; Xu, M.; Peng, J.B. Enhancement of tandem organic light-emitting diode performance by inserting an ultra-thin Ag layer in charge generation layer. *Acta Phys. Sin.* **2017**, *66*, 017302.
194. Li, J.; Shan, X.; Bade, S.G.R.; Geske, T.; Jiang, Q.; Yang, X.; Yu, Z. Single-Layer Halide Perovskite Light-Emitting Diodes with Sub-Band Gap Turn-On Voltage and High Brightness. *J. Phys. Chem. Lett.* **2016**, *7*, 4059–4066. [[CrossRef](#)] [[PubMed](#)]
195. Luo, D.; Chen, Q.; Qiu, Y.; Liu, B.; Zhang, M. Carbon Dots-Decorated Bi_2WO_6 in an Inverse Opal Film as a Photoanode for Photoelectrochemical Solar Energy Conversion under Visible-Light Irradiation. *Materials* **2019**, *12*, 1713. [[CrossRef](#)]
196. Liu, B.; Gao, H.; Hu, S.; Liu, C. Progress in the Development of Colloidal Quantum Well Light-Emitting Diodes. *Acta Phys. Chim. Sin.* **2022**, *38*, 2204052. [[CrossRef](#)]
197. Xiao, P.; Huang, J.; Dong, T.; Xie, J.; Yuan, J.; Luo, D.; Liu, B. Room-Temperature Fabricated Thin-Film Transistors Based on Compounds with Lanthanum and Main Family Element Boron. *Molecules* **2018**, *23*, 1373. [[CrossRef](#)]
198. Liu, B.; Delikanli, S.; Gao, Y.; Dede, D.; Gungor, K.; Demir, H.V. Nanocrystal light-emitting diodes based on type II nanoplatelets. *Nano Energy* **2018**, *47*, 115–122. [[CrossRef](#)]
199. Altintas, Y.; Liu, B.; Hernández Martínez, P.L.; Gheshlaghi, N.; Shabani, F.; Sharma, M.; Wang, L.; Sun, H.; Mutlugun, E.; Demir, H.V. Spectrally Wide-Range-Tunable, Efficient, and Bright Colloidal Light-Emitting Diodes of Quasi-2D Nanoplatelets Enabled by Engineered Alloyed Heterostructures. *Chem. Mater.* **2020**, *32*, 7874–7883. [[CrossRef](#)]
200. Luo, D.; Wang, L.; Qiu, Y.; Huang, R.; Liu, B. Emergence of Impurity-Doped Nanocrystal Light-Emitting Diodes. *Nanomaterials* **2020**, *10*, 1226. [[CrossRef](#)]
201. Ji, W.; Shen, H.; Zhang, H.; Kang, Z.; Zhang, H. Over 800% efficiency enhancement of all-inorganic quantum-dot light emitting diodes with an ultrathin alumina passivating layer. *Nanoscale* **2018**, *10*, 11103–11109. [[CrossRef](#)]

Disclaimer/Publisher's Note: The statements, opinions and data contained in all publications are solely those of the individual author(s) and contributor(s) and not of MDPI and/or the editor(s). MDPI and/or the editor(s) disclaim responsibility for any injury to people or property resulting from any ideas, methods, instructions or products referred to in the content.